Electronic Supplementary Material (ESI) for RSC Advances

Supporting Information

Highly Selective "*turn-off*" Fluorescent Sensing of Mercury Ion Using Aminocyclodextrin:3-Hydroxy-*N*-phenyl-2-naphthamide Complex in Aqueous Solution

Kuppusamy Kanagaraj,[a] Kasinathan Bavanidevi,[a] Tahsin J. Chow*[b] and Kasi Pitchumani*[a]

[a]*School of Chemistry, Madurai Kamaraj University, Madurai 625021, India*

[b]*Institute of Chemistry, Academia Sinica, Taipei 115, Taiwan*

***E-mail**: pit12399@yahoo.com and tjchow@chem.sinica.edu.tw

TABLE OF CONTENTS

1. General Information

1.1 Experimental

Materials

α-Cyclodextrin, *β*-Cyclodextrin, *γ*-Cyclodextrin and 3-Hydroxy-*N*-phenyl-2-naphthamide were purchased from Sigma Aldrich (India). All the cation salts such as $LiNO_3$, NaCl, KCl, $CaCl_2$, $AlCl_3$, $MgCl_2$, $CaCl_2$, $CrCl_3$, $MnCl_2$, $FeCl_3$, $FeCl_2$, $CoCl_2$, $NiCl_2$, $CuCl_2$, $ZnCl_2$, $PdCl_2$, $CdCl_2$, $InCl_3$, $SnCl_2$, $SbCl_3$, $HgCl_2$, $Hg(OAc)_2$, $Hg(ClO_4)_2$, $Hg(NO_3)_2$, $Pb(NO_3)_2$, $Bi(NO_3)_2$, $AgNO_3$ and the tetrabutylammonium (TBA) salts of various anions *viz.*, F^-, Cl^-, Br^-, I^-, CH_3COO^-, HSO_4^-, $H_2PO_4^-$ and ClO_4^- are used as received without further purification. Double distilled water (which was free from ions) and HPLC grade solvents were used for all spectral measurements. All other chemicals and solvents were purchased from Aldrich, Merck and used as received without further purification.

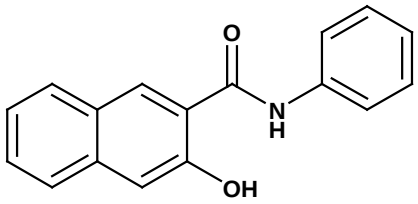

Figure S1. Structure of 3-hydroxy-N-phenyl-2-naphthamide (**2**)

1.2 Methods

^1H and ^{13}C NMR (Nuclear Magnetic Resonance) spectra were acquired on a Bruker DRX-300 (300 MHz) instrument using TMS as an internal standard. Data for ^1H NMR are recorded as follows: chemical shift (δ, ppm, parts per million), multiplicity (s = singlet, d = doublet, t = triplet, m = multiplet or unresolved, dd = doublet of doublet, br s = broad singlet, coupling constant(s) in Hertz (Hz), integration). Data for ^{13}C NMR are reported in terms of chemical shift (δ, ppm). Binding constants were calculated by non-linear regression using prism software (trial version) in an IBM compatible personal computer with Microsoft Windows XP service pack 2 operating system. All the absorption spectra were recorded in a JASCO V-550 double beam spectrophotometer with PMT detector. The emission spectra were recorded in a FLUOROMAX-4 spectrofluorometer (HORIBA JOBIN YVON) with excitation slit set at 2.0 nm bandpass and emission at 5.0 nm bandpass in 1 cm x 1 cm quartz cell. Induced Circular Dichroism (ICD) spectra were recorded in a JASCO J-810 spectropolarimeter with PMT detector, FT-IR were recorded in a JASCO FT/IR-410 spectrometer. DFT calculations were carried out at the B3LYP/LANL2DZ (d) level by using the

Gaussian 03 program. Electrospray Ionization Mass Spectrometry (ESI-MS) analysis were recorded in LCQ Fleet, Thermo Fisher Instruments Limited, US.

1.3 Preparation of stock solutions

Stock solution (1 x 10^{-4} M) of aminocyclodextrins (**1a-1f**) used for all sensing studies was prepared by dissolving respective amount (for **1b**, 0.0282 g) of aminocyclodextrin (**1a-1f**) in 250 mL of double distilled water and the solution was continuously sonicated for 12 h for complete solubilization, which guarantees solubility is <5 x 10^{-4} M. Stock solution (1 x 10^{-4} M) of 3-Hydroxy-*N*-phenyl-2-naphthamide (**2**) was prepared by dissolving 0.0066 g of **2** in 250 mL using ACN. All the cation solutions were prepared from $LiNO_3$, NaCl, KCl, $CaCl_2$, $AlCl_3$, $MgCl_2$, $CaCl_2$, $CrCl_3$, $MnCl_2$, $FeCl_3$, $FeCl_2$, $CoCl_2$, $NiCl_2$, $CuCl_2$, $ZnCl_2$, $PdCl_2$, $CdCl_2$, $InCl_3$, $SnCl_2$, $SbCl_3$, $HgCl_2$, $Hg(OAc)_2$, $Hg(ClO_4)_2$, $Hg(NO_3)_2$, $Pb(NO_3)_2$, $Bi(NO_3)_2$, and $AgNO_3$ in double distilled water, with a concentration of 2 x 10^{-3} M, respectively. All the anion solutions were prepared from tetrabutylammonium (TBA) salts of various anions *viz.*, F^-, Cl^-, Br^-, I^-, CH_3COO^-, HSO_4^-, $H_2PO_4^-$ and ClO_4^- in double distilled water, with a concentration of 2 x 10^{-3} M, respectively.

1.4 Determination of binding constant

Binding constants[S1] for the formation of binary (1:1) and ternary (1:2, 2:1) Host:Guest complex of aminocyclodextrin and 3-Hydroxy-*N*-phenyl-2-naphthamide were calculated by Benesi-Hildebrand and non-linear curve fitting method in 5% ACN:water mixture.

Benesi-Hildebrand[S2] equation (eqn. 1) was used to calculate the equilibrium constants for the 1:1 and 1:2 host:guest inclusion complexes formed between the substrate and the CD from UV studies.

$$\frac{[CD]\,[substrate]}{\Delta OD} = \frac{[CD] + [substrate]}{\Delta\varepsilon} + \frac{1}{K_f\,\Delta\varepsilon} \qquad \text{--- 1}$$

$$\{([CD]^2\,[substrate])/\Delta OD\}\ \text{Vs}\ \{[CD]^2\,[substrate]\} \qquad \text{--- 2}$$

In some of the cases the binding constant also calculated using the following equation 3 and 4 were applied for 1:1 and 1:2 complexation of guest with CD respectively.

$$\Delta OD = \frac{[\varepsilon_{SCD} - \varepsilon_{S_0}]\,K_1[CD][S_0]}{1 + K_1\,[CD]} \qquad \text{--- 3}$$

$$\Delta OD = \frac{[\varepsilon_{SCD} - \varepsilon_{S_0}]\,K_1[CD][S_0] + [\varepsilon_{S(CD)_2} - \varepsilon_{S_0}]K_1K_2[CD]^2[S_0]}{1 + K_1[CD] + K_1K_2[CD]^2} \qquad \text{--- 4}$$

where, ΔOD = absorbance value of the substrate in presence and absence of cyclodextrin; $[S]_0$ and [CD] are concentrations of substrate and cyclodextrins respectively; $\varepsilon_{S(CD)2}$, ε_{SCD} and ε_S are molar extinction coefficient of the complexes and substrate; K_1 and K_2 are binding constant values of the 1:1 and 1:2 guest and host complexes. These equations are solved by non-linear regression analysis using Graph pad PRISM (Trial software).

1.5 The fluorescent quantum yields (Φ)

Fluorescent quantum yields (Φ) of the probe **L1** (Φ_{L1}) and probe **L1**:Hg^{2+} complex ($\Phi_{L1:Hg}$) were compared, which was calculated using the fluorescent quantum of fluorescein as reference compound in 0.1 N NaOH solution (Φ_F = 0.79 %) *via* Eq. (5) and Eq. (6).[S3]

$$\Phi_{L1} = \Phi_F\left(\frac{Grad_F}{Grad_{L1}}\right)\left(\frac{\eta_{L1}^2}{\eta_F^2}\right) \quad \text{--- 5}$$

$$\Phi_{L1:Hg} = \Phi_F\left(\frac{Grad_F}{Grad_{L1:Hg}}\right)\left(\frac{\eta_{L1:Hg}^2}{\eta_F^2}\right) \quad \text{--- 6}$$

Where, Φ_{L1} and $\Phi_{L1:Hg}$ were the quantum yields of probe **L1** and the quantum yields of probe **L1**:Hg^{2+} complex; Φ_F is the quantum yields of reference dye fluorescein (0.1 N NaOH solution (Φ_F = 0.79 %), respectively. η_{L1} and $\eta_{L1:Hg}$ were the refractive indexes of the solvents of probe **L1** and probe **L1**:Hg^{2+} complex; η_F is the refractive indexes of the solvents of reference respectively.

2. Preparation and characterization of probe L1

2.1 Preparation and characterization of aminocyclodextrins

Aminocyclodextrins *viz.* per-6-amino-α-cyclodextrin (per-6-AACD, **1a**), per-6-amino-β-cyclodextrin (per-6-ABCD, **1b**), per-6-amino-γ-cyclodextrin (per-6-AGCD, **1c**), mono-6-amino-α-cyclodextrin (mono-6-AACD, **1d**), mono-6-amino-β-cyclodextrin (mono-6-ABCD, **1e**) and mono-6-amino-γ-cyclodextrin (mono-6-AGCD, **1f**) were synthesized and purified according to the procedure described in the literature.[S1] The product was dried for 24 h under vacuum over phosphorus pentoxide at 60 ^oC and then stored in a vacuum desiccators and are characterized by ^1H and ^{13}C-NMR, ESI-MS and elemental analysis, which are in accordance with literature reports.[S4]

Characterization of Per-6-amino-6-*β*-cyclodextrin (as its hydrochloride salt) (per-6-ABCD, 1b): pale yellow solid (98% yield); mp. 208 °C {lit.[S4] mp. 207-209 °C}. **^{1}H-NMR (300 MHz, D_2O, δ ppm):** 3.26 (dd, *J* = 7.1, 13 Hz, 7H); 3.44 (dd, *J* = 3, 13.2 Hz, 7H); 3.57 (t, *J* = 9.1 Hz, 7H); 3.64 (dd, *J* = 3.5, 9.5 Hz, 7H); 3.98 (dd, *J* = 9, 9.5 Hz, 7H); 4.15-4.25 (ddd, *J* = 3.1, 7, 9 Hz, 7H); 5.15 (d, *J* = 3.6 Hz, 7H) (Fig. S1); **^{13}C-NMR (75 MHz, D_2O, δ ppm):** 42.9; 70.5; 74.3; 74.8; 84.8; 104.1 (Fig. S2); **ESI-MS:** *m/z* Calcd. for $C_{42}H_{77}N_7O_{28}$ $[M+H]^+$: 1128.4895; Found, 1128.5102 (Rel. Int. 100%). **Elemental Analysis:** Calcd. for $C_{42}H_{77}N_7O_{28}$: C, 44.72; H, 6.88; N, 8.69; O, 39.71; Found: C, 44.73; H, 6.88; N, 8.70; O, 39.71.

2.2 Preparation and characterization of probe L1

General procedure for preparation of sensing probe L1

Stock solutions (1 x 10^{-4} M) of per-6-ABCD (**1b**) were prepared by dissolving 0.0282 g, 250 mL SMF using double distilled water and the solution was continuously sonicated for 12 h for complete solubilization. Stock solution of 3-Hydroxy-*N*-phenyl-2-naphthamide (**2**) (0.0066 g) were prepared separately in 250 mL SMF using 5% ACN:water mixture. 5% ACN Aqueous solution of the per-6-ABCD:**2** complex (**1b**:**2**, probe **L1**) was prepared *in situ* from the reaction of **1b** (1 x 10^{-4} M) and **2** (1 x 10^{-4} M) by stirring for 6 h at room temperature. Probe **L1** was characterized by UV-Vis., fluorescence, NMR, ESI-MS and Job's plot.

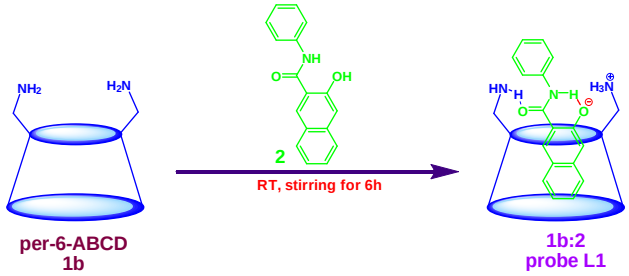

Scheme S1. Preparation of probe **L1**

2.3 Spectral characterization of probe L1

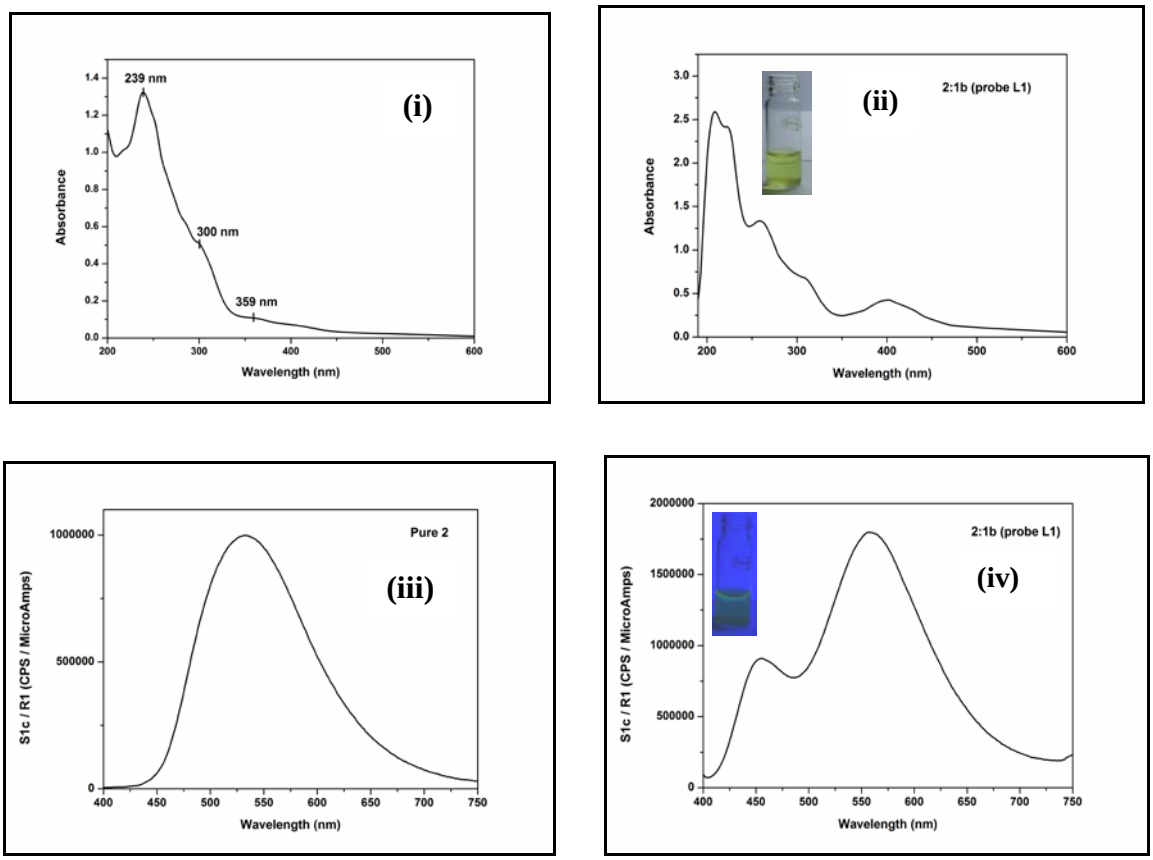

Figure S2. UV-Vis., absorption spectra of (i) **2** (λ_{abs} = 359, 300 and 239 nm) and (ii) probe **L1** (λ_{abs} = 400, 312, 255, 224 and 208 nm) and fluorescence spectra of (iii) **2** (λ_{exc} = 360 nm) and (iv) probe **L1** (λ_{exc} = 400 nm) in 5% ACN:water mixture; [**2**] and [probe **L1**] = 60 μM.

Figure S2(i) and (ii) show the UV-Vis. absorption and fluorescence spectra of **2** (60 μM), which exhibit absorption maxima at 359, 300 and 239 nm and a relatively short wave length emission (λ_{exc} = 360 nm) which appears at 533 nm (λ_{emi}) with optimal intensity (Schemes S2 and S3). Florescence emission intensity is increased upon equimolar addition of β-CD and there is no significant change in emission wavelength.

Fluorescence emission intensity of **2** is enhanced upon equimolar addition of β-CD in 5% ACN:water mixture, whereas upon addition of per-6-ABCD (**1b**) to **2**, two distinct emission bands are observed with red shift (band I: 463 nm and band II: 577 nm) with high fluorescence intensity. This observation due to the localized emission of naphthyl group in per-6-ABCD cavity for band I and the band II for the PET process from naphthyl group to phenyl group, in which **2** binds to **1b** in the ground state through hydrogen bonding

interaction *via* amino groups of **1b** and OH group of **2**. Upon complexation with **1b** co-planarity was achieved, which is confirmed from molecular modeling studies (see Molecular moldeling study).

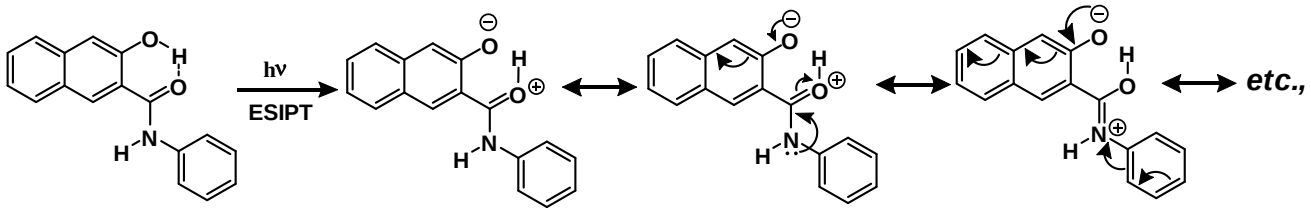

Scheme S2. ESIPT process in uncomplexed state.

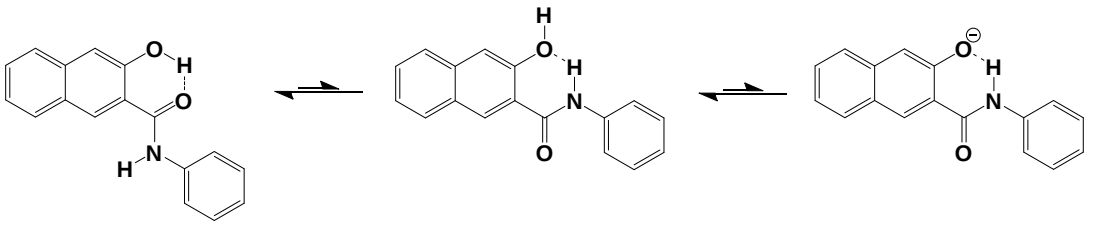

Scheme S3. Various ionic forms of **2** at different solvents and pH values.

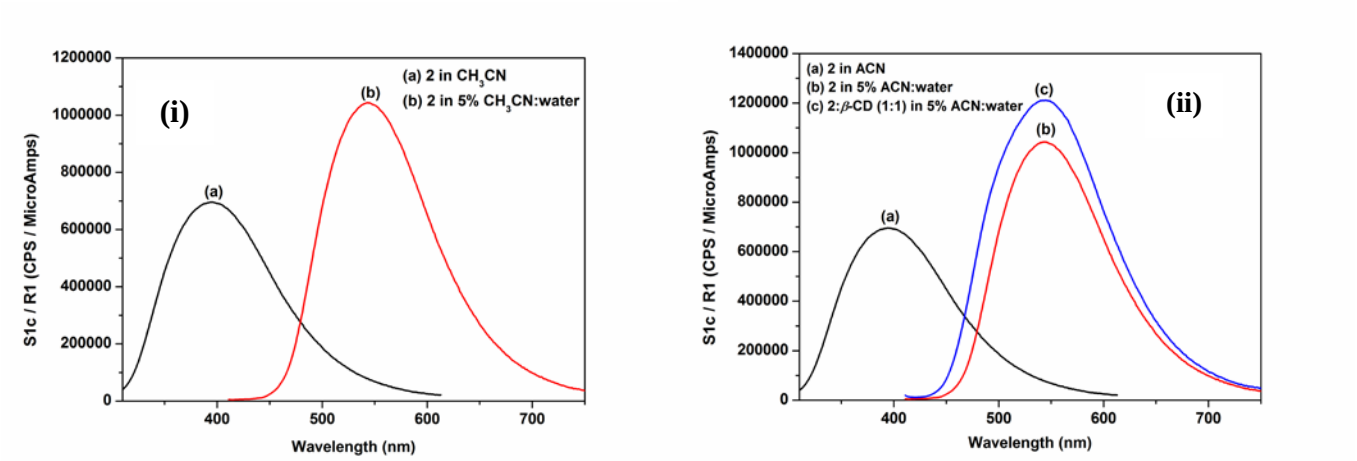

Figure S3. (i) and (ii) Fluorescence spectra of **2** (60 μM) in 5% ACN:water mixture ((a) λ_{exc} = 300 nm; λ_{emi} = 392 nm; (b), (c) λ_{exc} = 360 nm; λ_{emi} = 533 nm).

Jiang *et. al.*, reported[S5] that the 3-hydroxy-*N*-phenyl-2-naphthamide **2** has a short-wavelength fluorescence at 392 nm (λ_{exci} = 300 nm) with a very low fluorescence quantum yield ($\Phi \sim 10^{-4}$) in CH_3CN. Proton transfer occurs between hydroxyl and C=O groups (proton transfer from OH group to C=O group) (Scheme S2, form I). Whereas red shifted fluorescence observed at 533 nm (λ_{exci} = 360 nm) in 5%

ACN:water mixture, it is due to that proton transfer between hydroxyl group and NH group (proton transfer from NH group to OH group) (Scheme S2, form II). Red shifted fluorescence with higher quantum yield is observed in basic medium, it is due to proton transfer from NH group to O^- (linear form, high electron delocalization, solution in yellow color) (Scheme S2, form II).

2.4 Determination of binding constant of 2 with per-6-ABCD (1b)

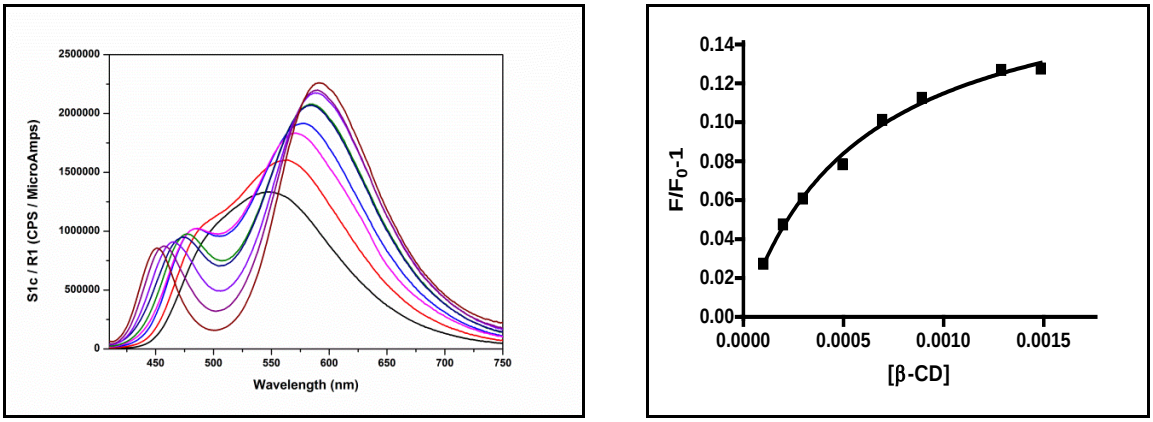

Figure S4. (a) Emission spectrum and (b) binding constant curve (calculated by non-linear curve fitting method) for **2** with per-6-ABCD (**1b**) in 5% ACN:water mixture; [**2**] = 60 μM, [**1b**] is varied from 0 to 150 mM

2.5 Job's plot for per-6-ABCD (1b) and 2

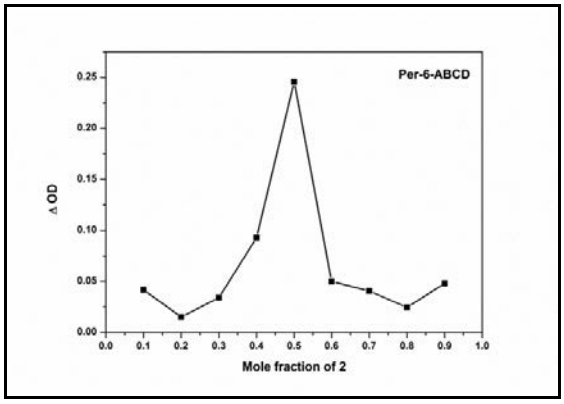

Figure S5. Job's plot for per-6-ABCD **1b** with **2** in 5% ACN:water mixture; [**2**] = 0 to 60 μM; [**1b**] = 0 to 60 μM.

3. NMR spectral studies

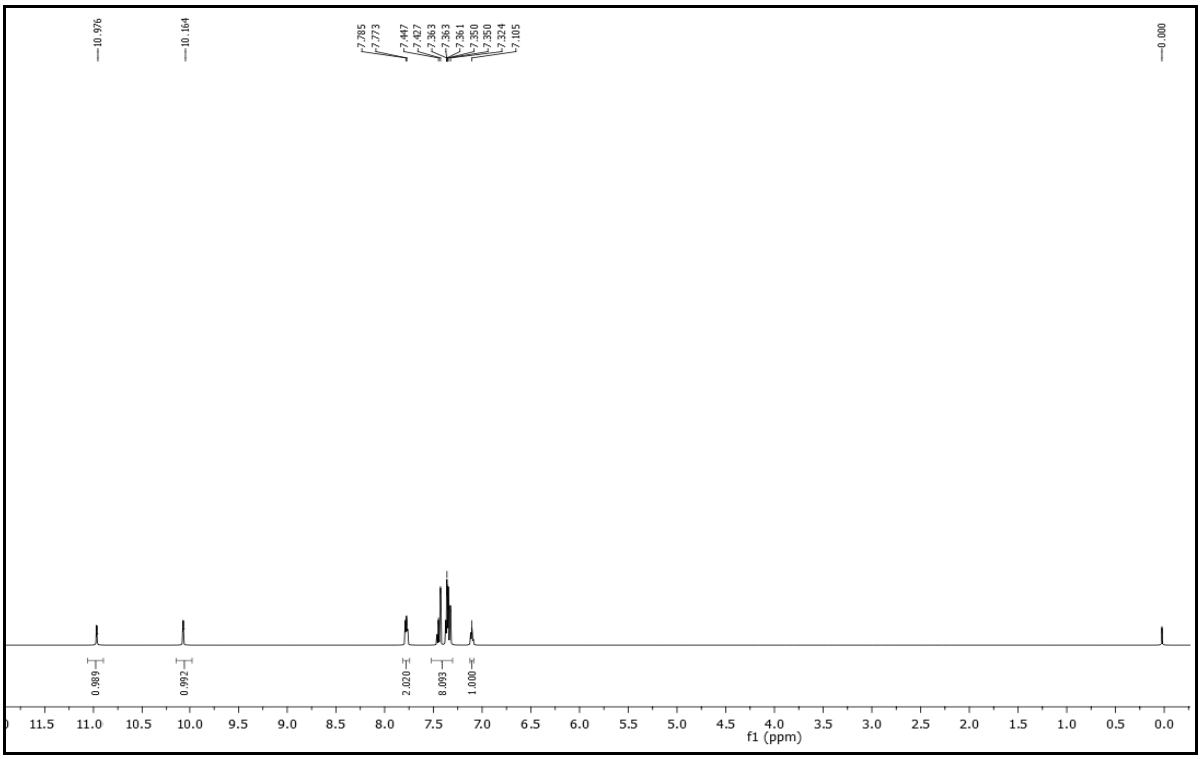

Figure S6. ^{1}H NMR (400 MHz) spectra of **2** in DMSO-d_6 in the absence of **1b**.

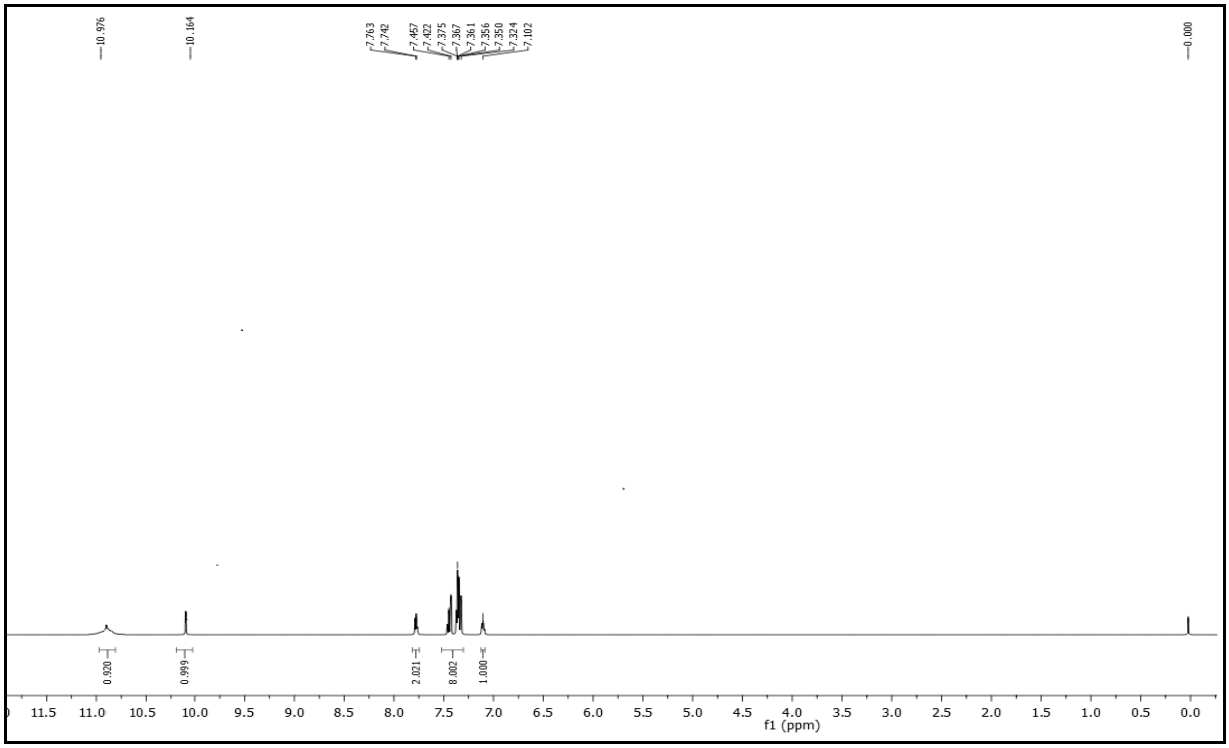

Figure S7. ^{1}H NMR (400 MHz) spectra of **2** in D_2O + 5% DMSO-d_6 in the absence of **1b**.

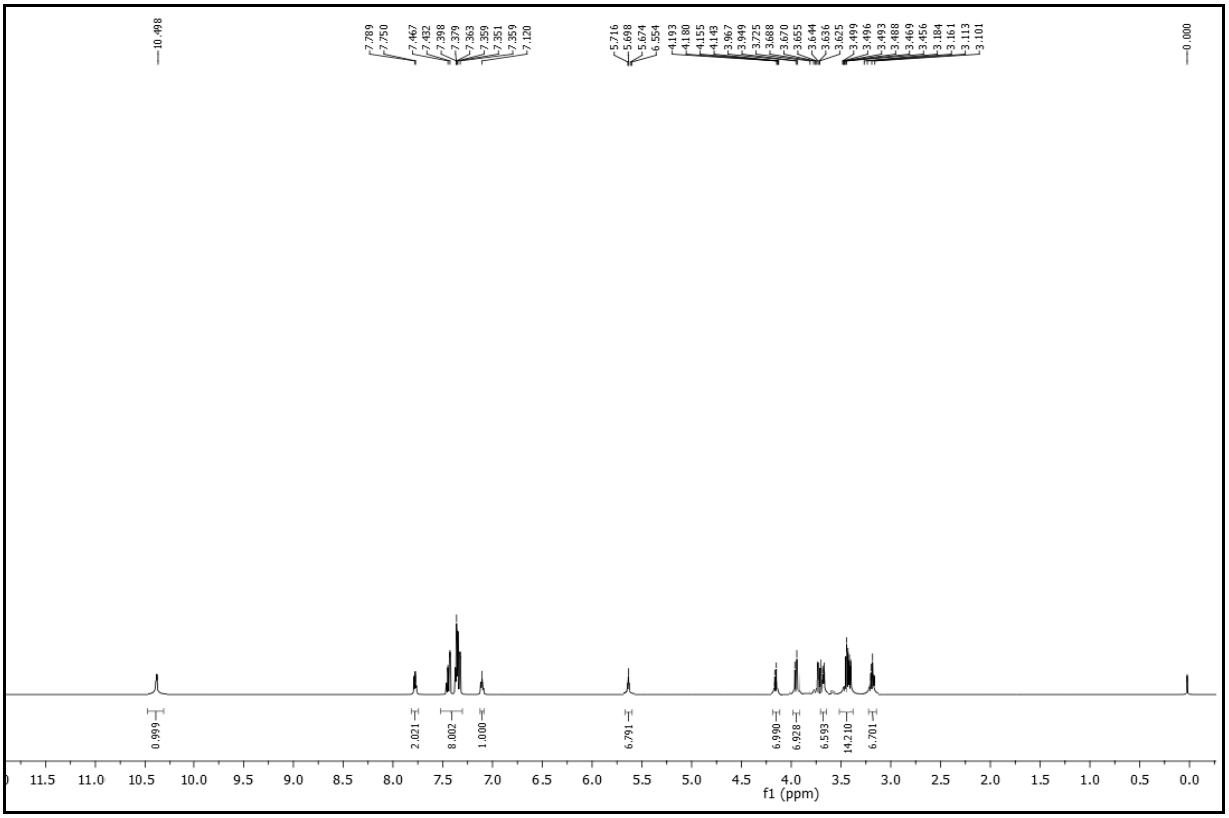

Figure S8. ^{1}H NMR (400 MHz) spectra of **2** in D_2O + 5% DMSO-d_6 in the presence of 0.5 equivalent of **1b**.

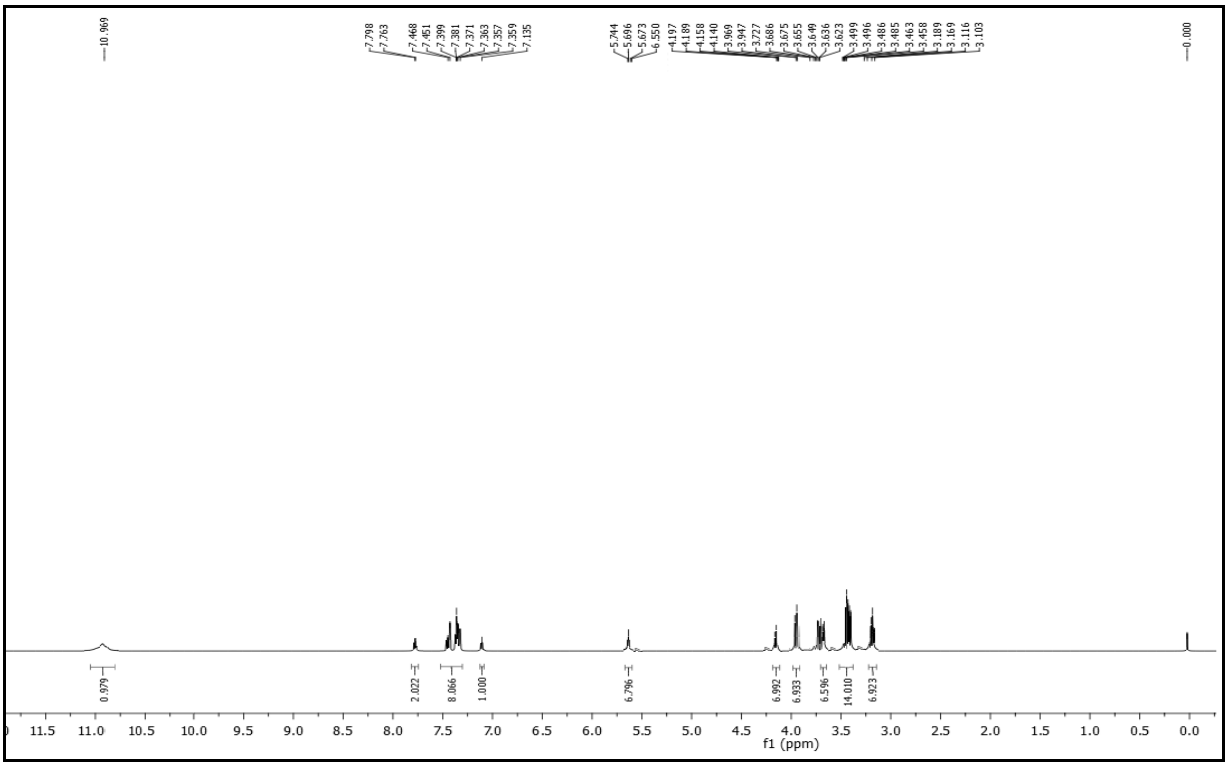

Figure S9. ^{1}H NMR (400 MHz) spectra of **2** in D_2O + 5% DMSO-d_6 in the presence of 1 equivalent of **1b**.

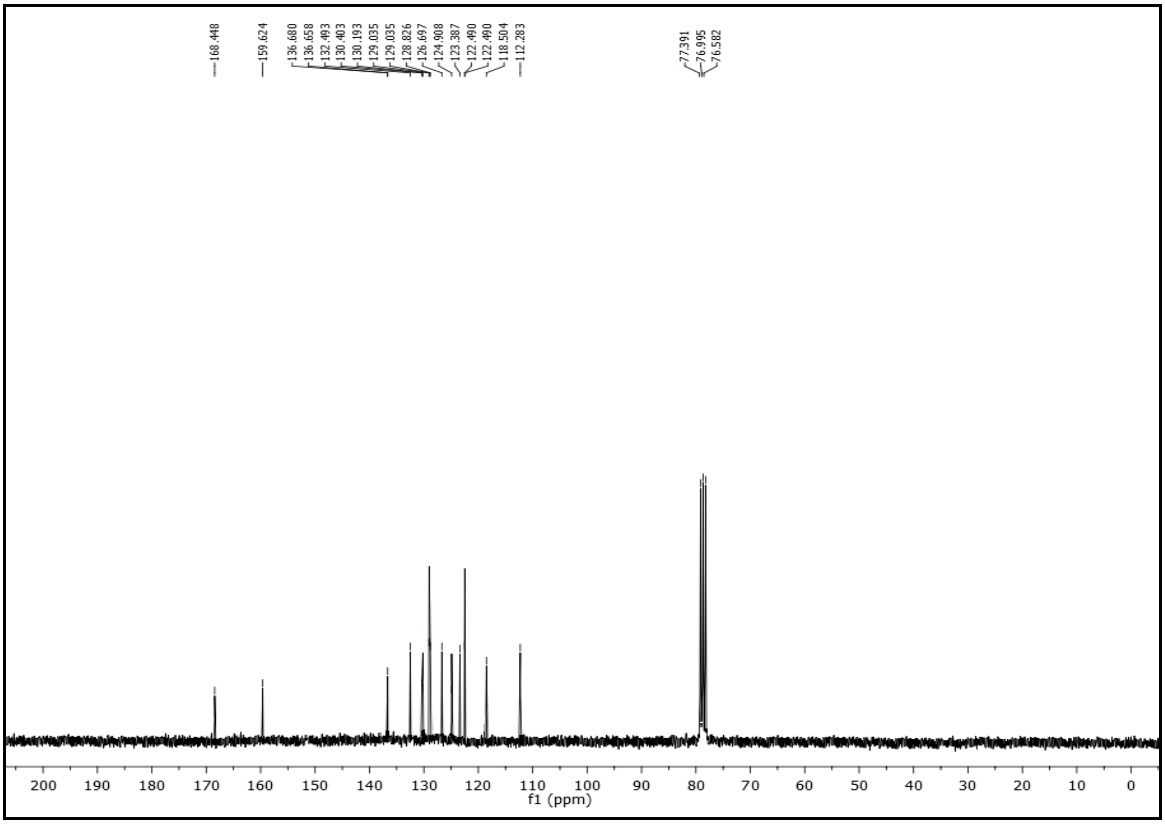

Figure S10. ^{13}C NMR (100 MHz) spectra of **2** with Hg^{2+} in DMSO-d_6.

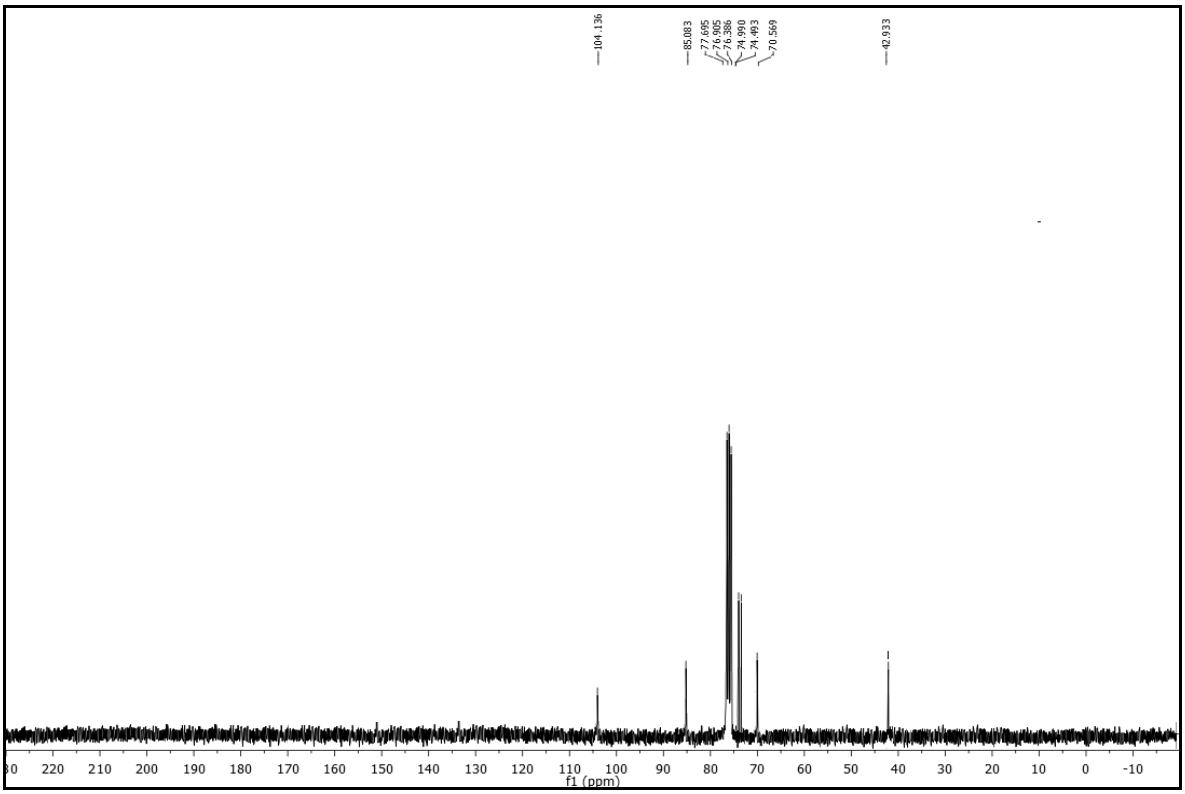

Figure S11. ^{13}C NMR (100 MHz) spectra of **1b** with Hg^{2+} in DMSO-d_6.

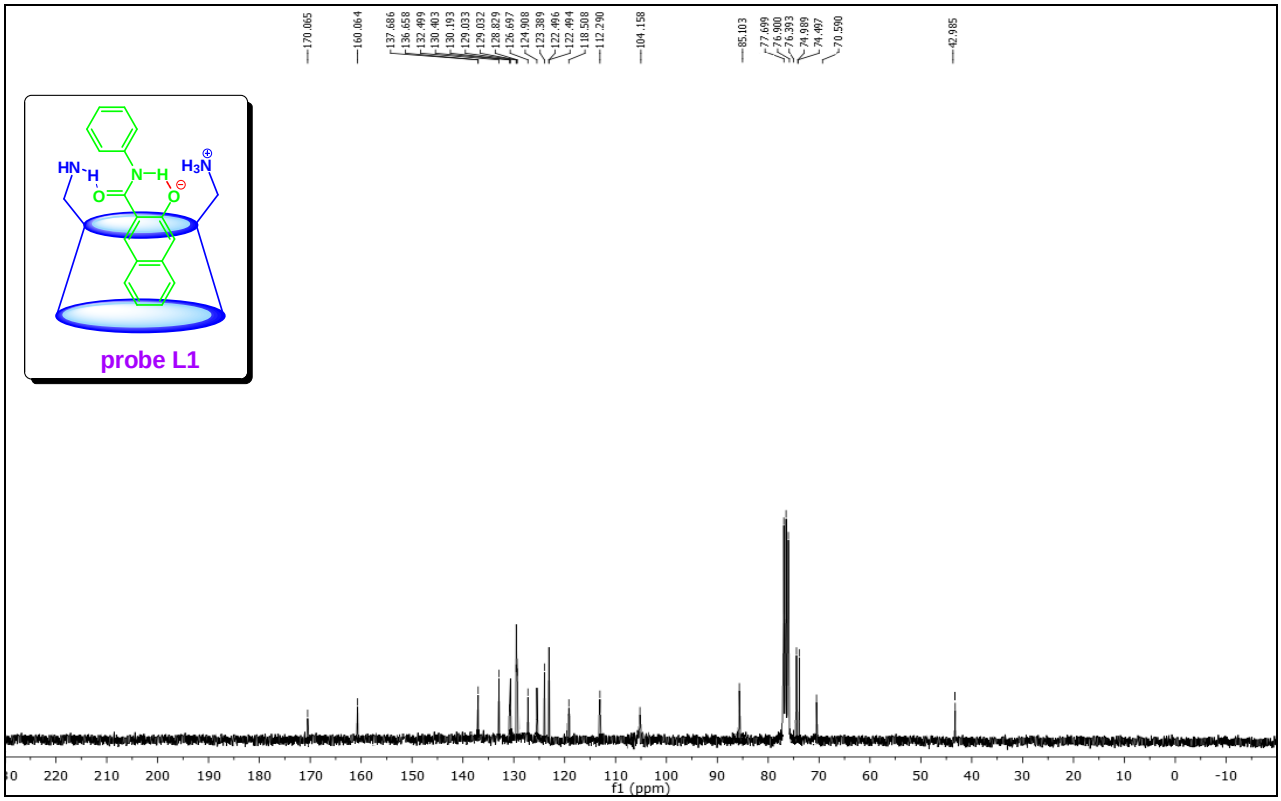

Figure S12. ^{13}C NMR (100 MHz) spectra of probe **L1** in DMSO-d_6.

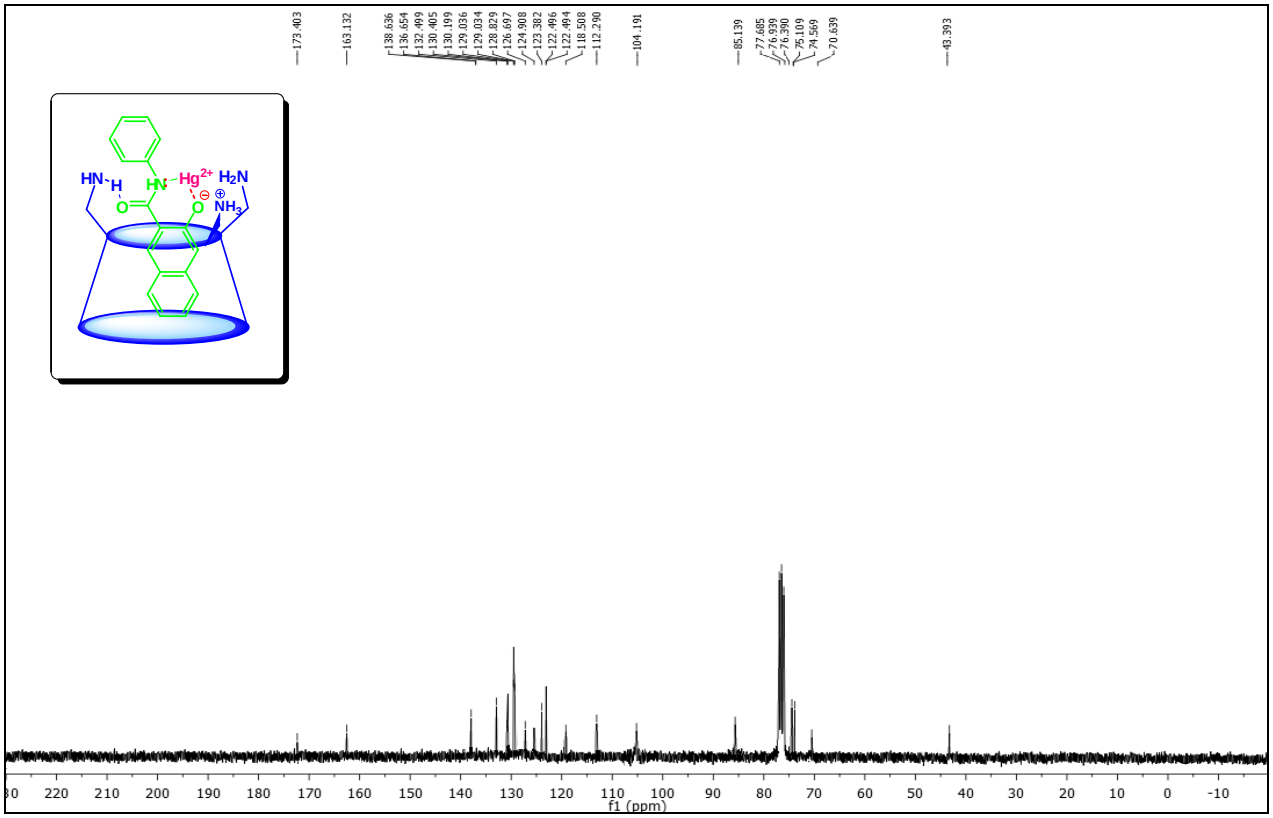

Figure S13. ^{13}C NMR (100 MHz) spectra of probe **L1**: Hg^{2+} complex in DMSO-d_6.

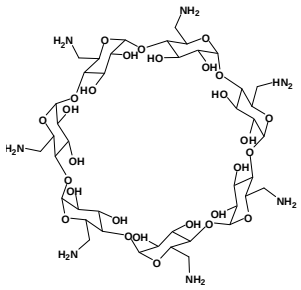

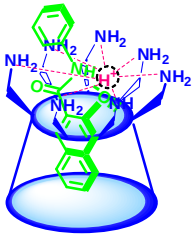

1b:2
probe L1

^{1}H-NMR (300 MHz, D_2O, δ ppm): 3.34 (dd, *J* = 7.4, 13.4 Hz, 7H), 3.49 (dd, *J* = 3.4, 13.3 Hz, 7H), 3.59 (t, *J* = 9.7 Hz, 7H), 3.72 (m, 7H), 4.15 (dd, *J* = 9.7, 9.5 Hz, 7H), 4.17-4.34 (m, 7H), 5.22 (d, *J* = 4.0 Hz, 7H), 7.24-7.43 (m, 1H), 7.51-7.71 (m, 7H), 7.89-7.93 (m, 2H), 8.51 (s, 1H), 10.23 (br s, 1H); **^{13}C-NMR (75 MHz, D_2O, δ ppm):** 43.4, 70.7, 74.7, 75.5, 85.1, 105.2, 111.9, 121.7, 122.0, 124.7, 125.8, 126.2, 128.1, 128.4, 128.6, 128.9, 129.2, 129.8, 130.1, 136.8, 137.7, 156.1, 165.4; **ESI-MS:** *m/z* calcd for $C_{59}H_{91}N_8O_{30}$, [**1b**:**2**], $[M+H]^+$:1391.58; Found, 1391.72 (Rel. Int. 100%). **Elemental Analysis:** Calcd. for $C_{59}H_{91}N_8O_{30}$: C, 38.86; C, 50.93; H, 6.52; N, 8.05; O, 34.50; Found: C, 50.95; H, 6.54; N, 8.07; O, 34.52.

4. Molecular modeling studies

Energy minimization studies

Energy minimized geometries of the complexes were obtained using Molecular Mechanics Calculations by INSIGHT II/DISCOVER program.[S6–S8] The initial structures of host and guest molecules were constructed by INSIGHT II/DISCOVER on Silicon Graphics IRIS workstation. We have adapted CVFF/AMBER force field to express the MM energies of per-6-ABCD (**1b**) host, 3-hydroxy-*N*-phenyl-2-naphthamide (**2**) and their complexes. Structures were minimized using CVFF force field and RMS derivative 0.001 was achieved in each case. Complexation energies were calculated using the following equation: $\Delta E = \Delta E_{Complex} - \Delta E_{Host} - \Delta E_{Guest}$.

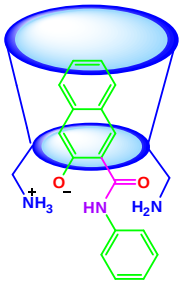

Mode Ia
ΔE = -76.9236 kcal. M^{-1}

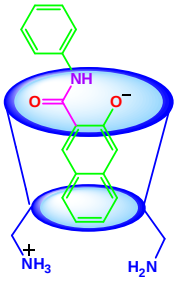

Mode Ib
ΔE = -27.4539 kcal. M^{-1}

Mode I: Naphthyl part is inside the CD-cavity and Phenyl part is outside the CD-cavity.

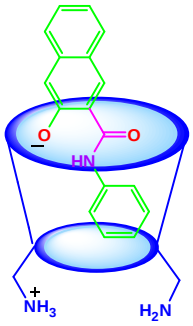

Mode Ia
ΔE = -18.6734 kcal. M^{-1}

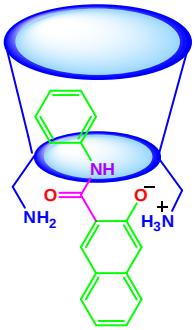

Mode Ib
ΔE = -44.1621 kcal. M^{-1}

Mode II: Phenyl part is inside the CD-cavity and Naphthyl part is outside the CD-cavity.

Figure S14. Possible mode of inclusion complex of per-6-ABCD (**1b**) with 3-hydroxy-*N*-phenyl-2-naphthamide (**2**); In mode Ia and Ib: naphthyl part is inside the CD-cavity and phenyl part is outside the CD-cavity; In mode IIa and IIb: phenyl part is inside the CD-cavity and naphthyl part is outside the CD-cavity.

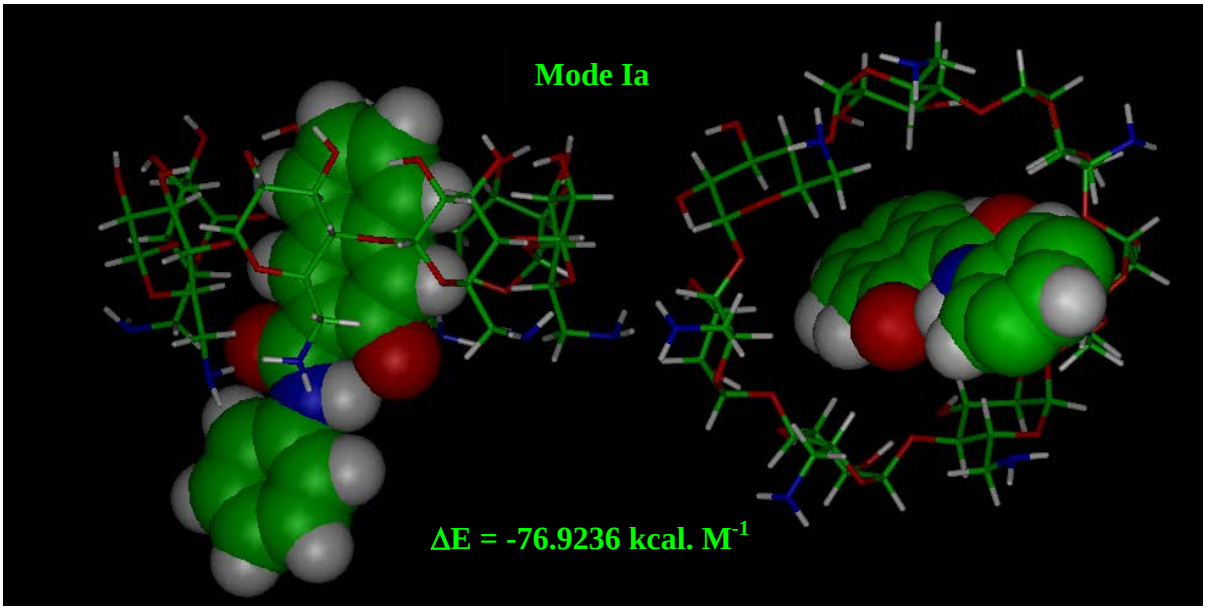

Figure S15. AMBER-optimized inclusion complex of per-6-ABCD (**1b**) with 3-hydroxy-*N*-phenyl-2-naphthamide (**2**); In mode Ia: Naphthyl part is inside the CD-cavity and Phenyl part is outside the CD-cavity (near to narrower rim of CD).

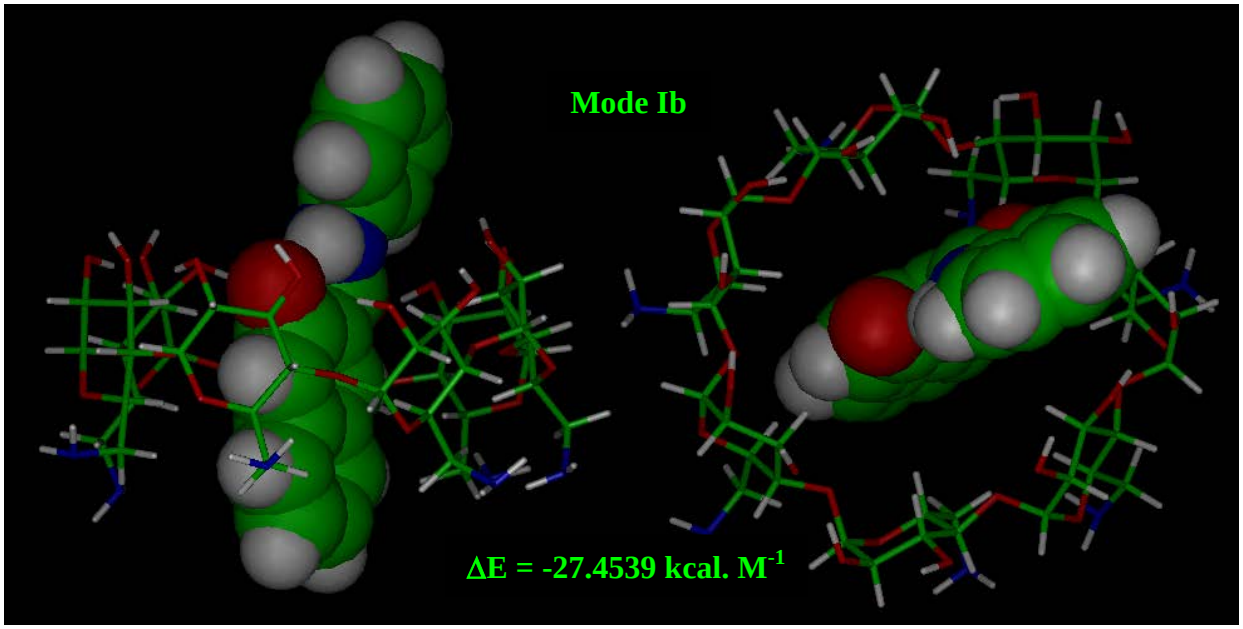

Figure S16. AMBER-optimized inclusion complex of per-6-ABCD (**1b**) with 3-hydroxy-*N*-phenyl-2-naphthamide (**2**); In mode Ib: Naphthyl part is inside the CD-cavity and Phenyl part is outside the CD-cavity (near to wider rim of CD).

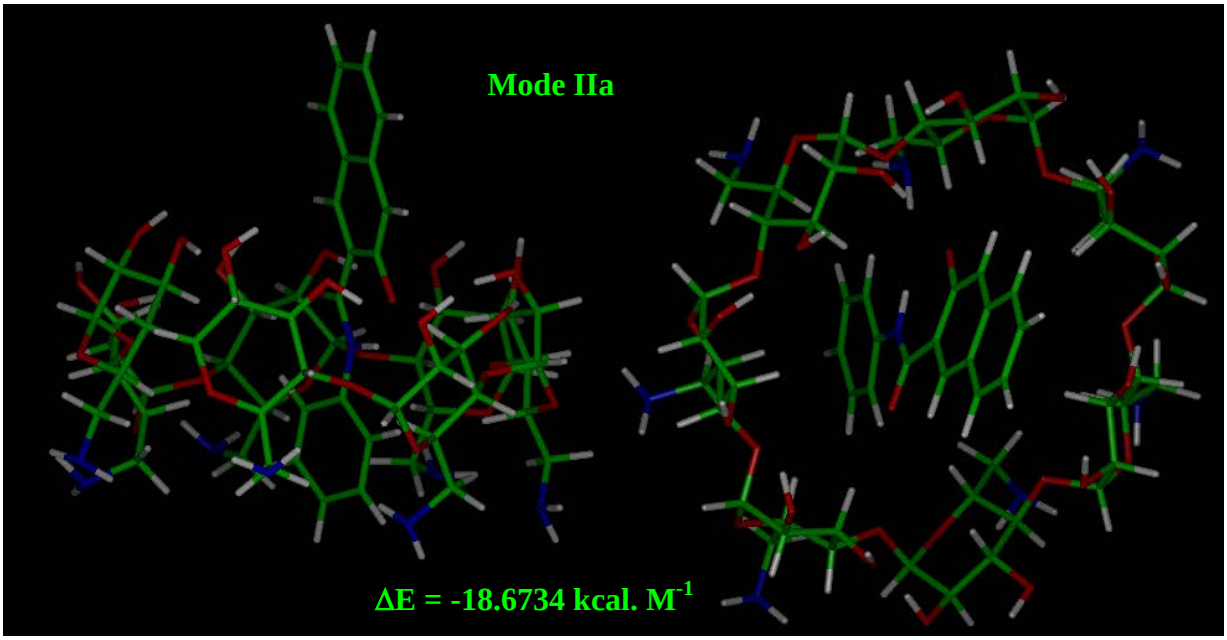

Figure S17. AMBER-optimized inclusion complex of per-6-ABCD (**1b**) with 3-hydroxy-*N*-phenyl-2-naphthamide (**2**); In mode IIa: Phenyl part is inside the CD-cavity and Naphthyl part is outside the CD-cavity (near to narrower rim of CD).

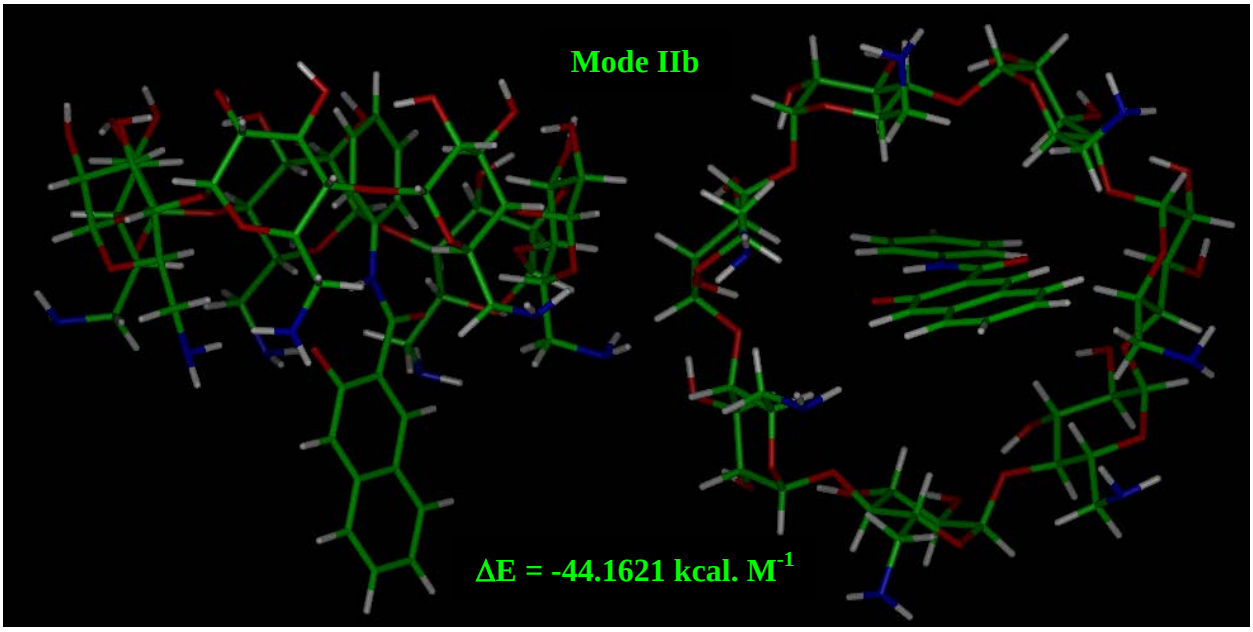

Figure S18. AMBER-optimized inclusion complex of per-6-ABCD (**1b**) with 3-hydroxy-*N*-phenyl-2-naphthamide (**2**); In mode IIa: Phenyl part is inside the CD-cavity and Naphthyl part is outside the CD-cavity (near to wider rim of CD).

5. DFT calculations[S9]

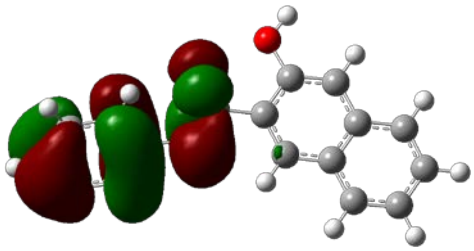

HOMO picture of 2

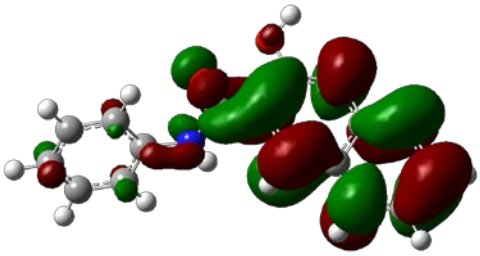

LUMO picture of 2

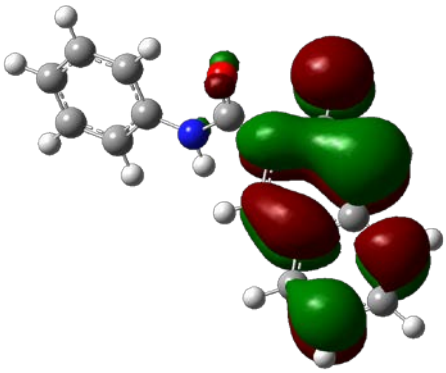

HOMO picture of 2 (anion)

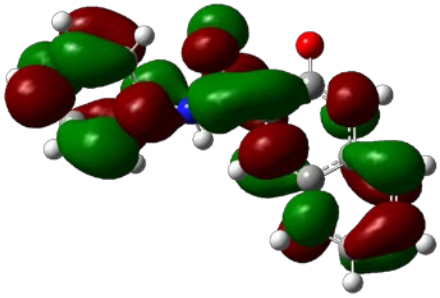

LUMO picture of 2 (anion)

Figure S19. Optimized geometries and HOMO–LUMO pictures of the 3-hydroxy-*N*-phenyl-2-naphthamide (**2**) and its anionic form (deprotonated form).

6. Selective sensing of Hg^{2+} ion

5.1 Binding constant measurements

Binding constant of various metal cations with probe **L1** are calculated by non-linear curve fitting method.[S7] Binding constant of various metal ions with probe **L1** were presented in table S1.

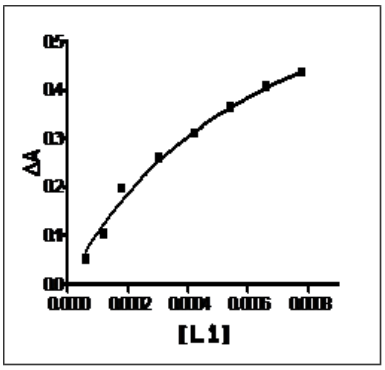

Figure S20. Non-linear curve fit binding constant plot for probe **L1** with Hg^{2+} ion.

Table S1. Binding constants of probe **L1** with various metal ions at room temperature

Probe	Metal ions	Binding constants[a] K_b (M^{-2})	Probe	Metal ions	Binding constants[a] K_b (M^{-2})
L1	Li^+	1023	**L1**	Pd^{2+}	3992
L1	Na^+	1137	**L1**	Cd^{2+}	4572
L1	K^+	1204	**L1**	Sn^{2+}	1093
L1	Ag^+	3123	**L1**	Hg^{2+}	9769
L1	Mg^{2+}	2045	**L1**	Pb^{2+}	1974
L1	Ca^{2+}	2134	**L1**	Al^{3+}	3643
L1	Mn^{2+}	1945	**L1**	Cr^{3+}	1834
L1	Fe^{2+}	3765	**L1**	Fe^{3+}	2912
L1	Co^{2+}	2391	**L1**	In^{3+}	1098
L1	Ni^{2+}	2121	**L1**	Sb^{3+}	1009
L1	Cu^{2+}	4896	**L1**	Bi^{3+}	1164
L1	Zn^{2+}	3465	**L1**	Pd^{2+}	3992

[a]K_b values are calculated from UV-Vis absorption data using non-linear curve fit binding constant plots.

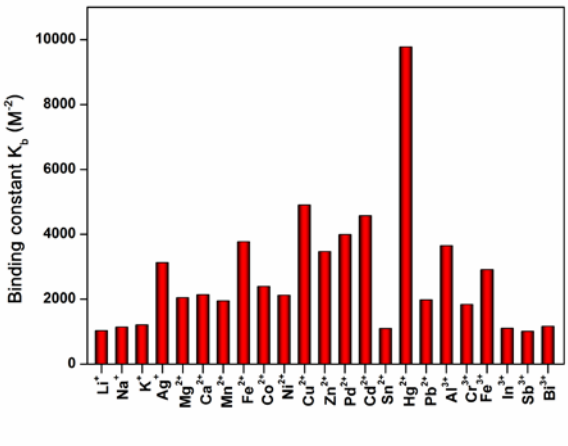

Figure S21. The binding constant of probe **L1** with various metal ions ($[M^{n+}] = 1 \times 10^{-5}$) in aqueous medium at room temperature.

Binding constant of **2** with various aminocyclodextrins (**1a-1f**) are calculated by non-linear curve fitting method.[S7] Binding constant of **2** with various aminocyclodextrins (**1a-1f**) were presented in table S2.

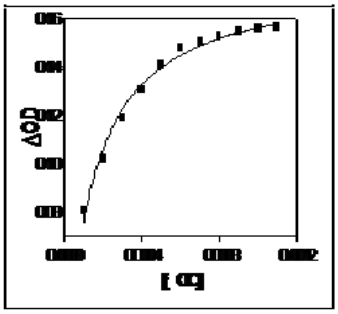

Figure S22. Non-linear curve fit binding constant plot for Per-6-ABCD, **1b** with **2**.

Table S2. Binding constants of **2** with various aminocyclodextrins (**1a-1f**) at room temperature

Aminocyclodextrins	**Binding constants[a] K_b (M^{-1})**
Per-6-AACD, **1a**	7347
Per-6-ABCD, **1b**	9769
Per-6-AGCD, **1c**	10692
Mono-6-AACD, **1d**	1921
Mono-6-ABCD, **1e**	2896
Mono-6-AGCD, **1f**	3325

[a]K_b values are calculated from UV-Vis absorption data using non-linear curve fit plots.

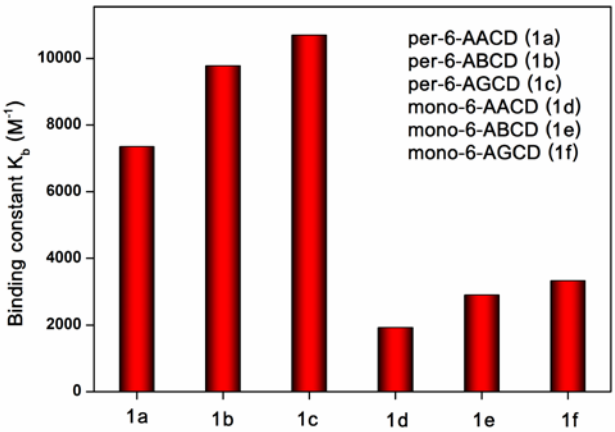

Figure S23. The binding constant of various aminocyclodextrins (**1a-1f**) ([**1a-1f**] = 1 x 10^{-5}) with **2** (0 to 1 x 10^{-4}) in aqueous medium at room teperature.

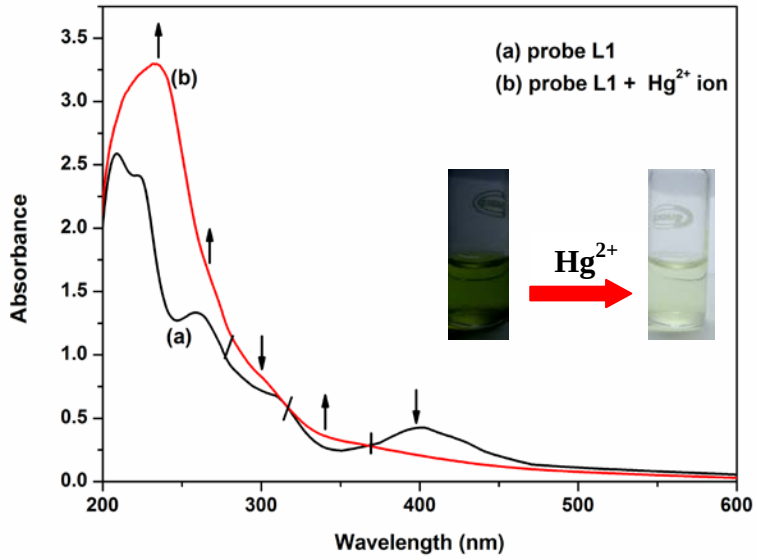

Figure S24. UV-Vis. absorption spectra of probe **L1** (60 μM) in the absence and presence of Hg^{2+} ion in 5% ACN:water mixture [Hg^{2+}] = 60 μM, [probe **L1**] = 60 μM, Inset: Color changes in probe **L1** upon addition of Hg^{2+} ion.

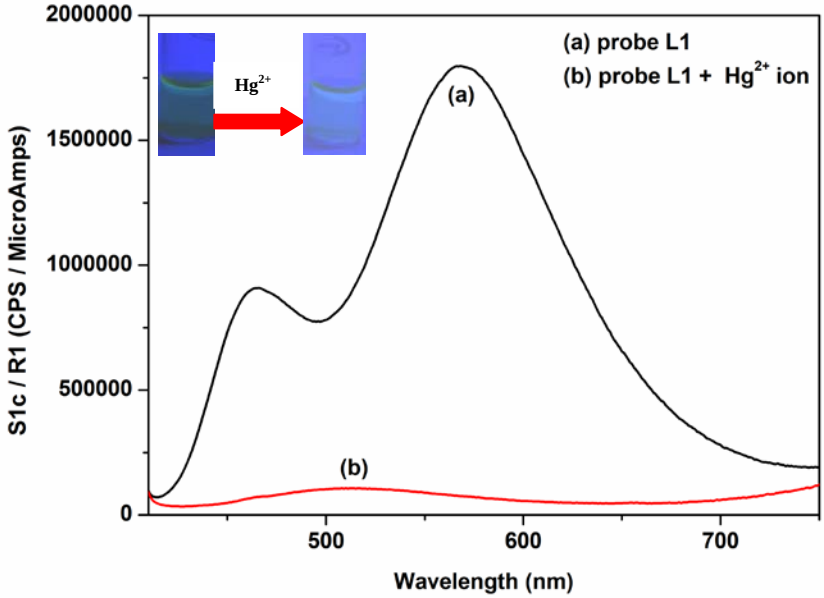

Figure S25. Fluorescence spectra of probe **L1** (60 μM) in the absence and presence of Hg^{2+} ion in 5% ACN:water mixture (λ_{exc} = 400 nm; λ_{emi} = 577 - 509 nm; Slit 5.0 nm/5.0 nm). Inset: Fluorescence changes excited by UV lamp (365 nm) in probe **L1** upon addition of Hg^{2+} ion.

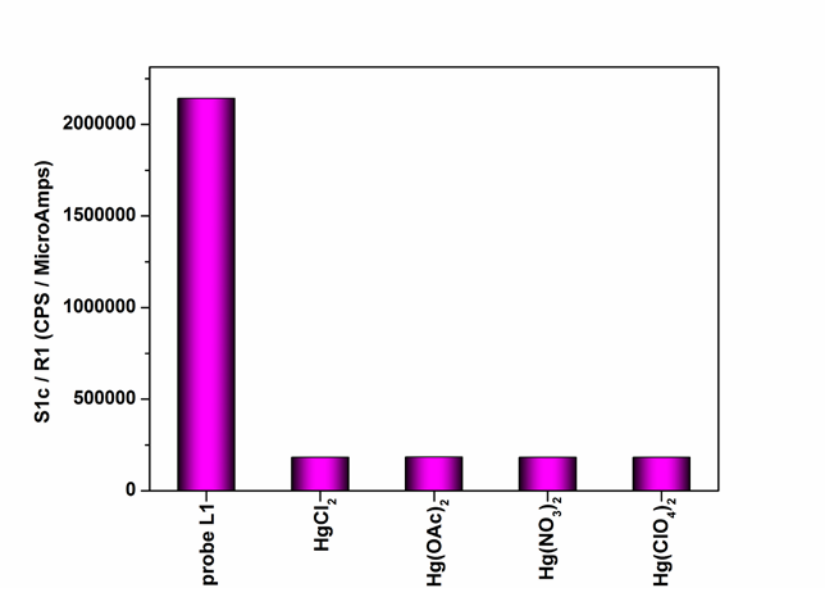

Figure S26. Fluorescence response of probe **L1** (60 mM) to various mercury metal sources (60 μM) *viz.*, $HgCl_2$, $Hg(OAc)_2$, $Hg(NO_3)_2$ and $Hg(ClO_4)_2$ in 5% ACN:water mixture. Bars represent the fluorescence response of probe **L1** in the absence and presence of mercury metal sources (60 μM) (λ_{exc} = 400 nm; λ_{emi} = 558 - 512 nm; Slit 5.0 nm/5.0 nm).

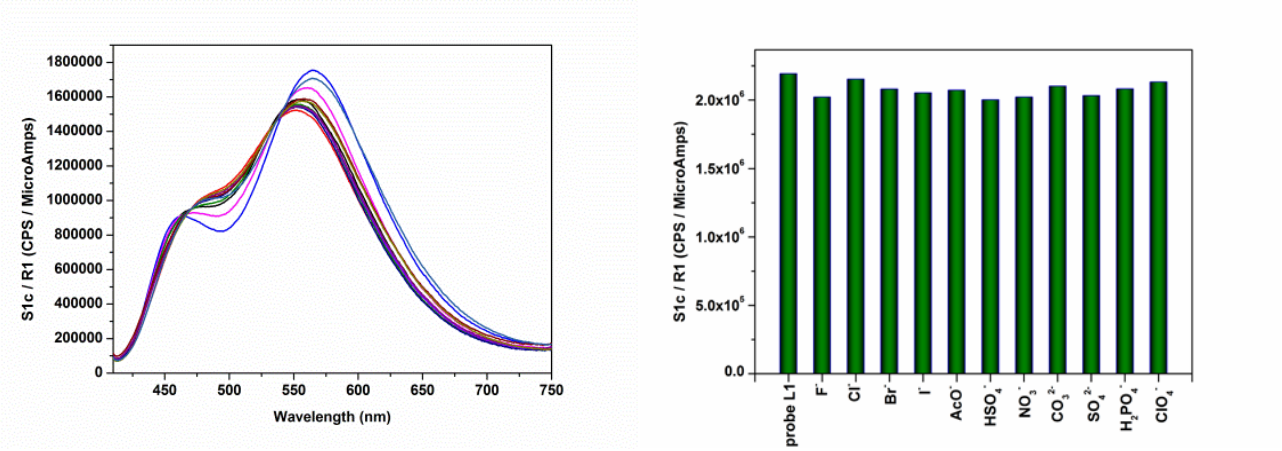

Figure S27. Fluorescence response of probe **L1** (60 μM) in the absence and presence of various anions (60 μM) *viz.*, F^-, Cl^-, Br^-, I^-, AcO^-, HSO_4^-, NO_3^-, CO_3^{2-}, SO_4^{2-}, $H_2PO_4^-$ and ClO_4^- (as their TBA salts) in 5% ACN:water mixture. Bars represent the fluorescence response of probe **L1** in the presence and absence of various anions (60 μM) (λ_{exc} = 400 nm; λ_{emi} = 558 nm; Slit 5.0 nm/5.0 nm).

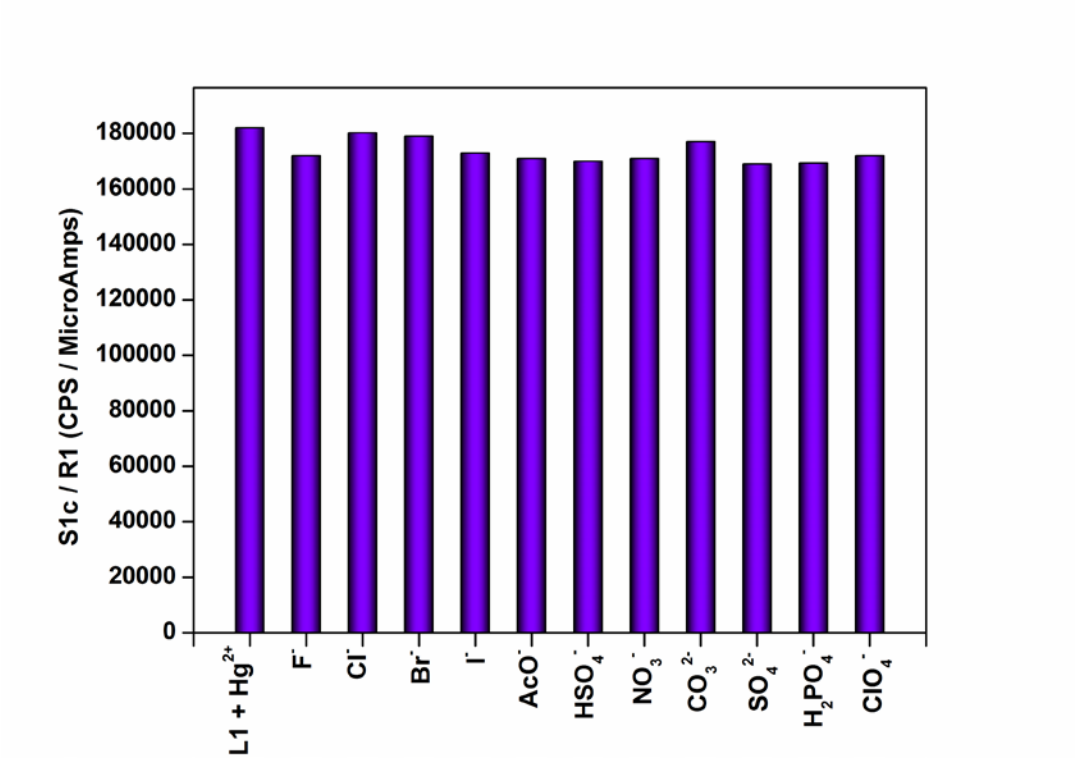

Figure S28. Fluorescence response of probe **L1**-Hg^{2+} complex (60 μM) in the absence and presence of 10 equivalents various anions (60 μM): F^-, Cl^-, Br^-, I^-, AcO^-, HSO_4^-, NO_3^-, CO_3^{2-}, SO_4^{2-}, $H_2PO_4^-$ and ClO_4^- (as their TBAB salts) in 5% ACN:water mixture. Bars represent the fluorescence response of probe **L1**-Hg^{2+} complex in the presence and absence of various anions (60 μM) (λ_{exc} = 400 nm; λ_{emi} = 577 - 509 nm; Slit 5.0 nm/5.0 nm).

5.2 Determination of LOD and LOQ

The detection limit was calculated based on the fluorescence titration. The fluorescence emission spectrum of probe **L1** was measured by four times and the standard deviation of blank measurement was achieved. To gain the slope of the fluorescence intensity maximum from 577-509 nm was plotted as a concentration of Hg^{2+} ion. So the detection limit was calculated with the following equivation:

$$\text{Limit of Detection (LOD)} = 3\sigma/k$$

Where σ is the standard deviation of blank measurement, k is the slope between the fluorescence intensity ratios versus $[Hg^{2+}]$

The Limit of Detection (LOD) for probe **L1** to Hg^{2+} were deduced to be 1×10^{-12} M (ppb).

The Limit of Detection (LOD) for probe **L2** to Hg^{2+} were deduced to be 2×10^{-10} M (ppb).

7. Control experiments

A similar spectral variations are observed with **2** (60 μM) in 5% ACN:water in the presence of an organic base (60 μM) (triethylamine and aq. NH_3), inorganic bases (60 μM) ($NaHCO_3$, Na_2CO_3 and NaOH) and in *aq.* NH_3/NH_4Cl buffer (pH = 8.5). Complete disappearance of characteristic UV-Vis. absorption maxima and fluorescence emission is noticed upon addition of *aq.* HCl solution into **2** (60 μM) in 5% ACN:water mixture.

Sensing response of probe L2-L6 with Hg^{2+} ions

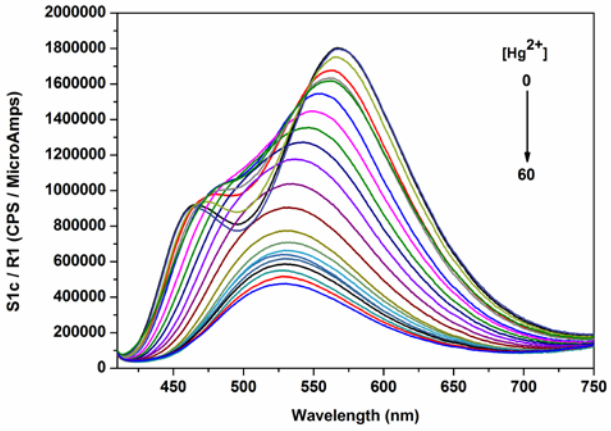

Figure S29. Fluorescence spectra of probe **L2** (60 μM) upon titration by Hg^{2+} ion (0-60 μM) in 5% ACN:water mixture, (λ_{exc} = 400 nm; λ_{emi} = 567 - 530 nm, $\Delta\lambda_{emi}$ = 37 nm, Slit: 5 nm/5 nm).

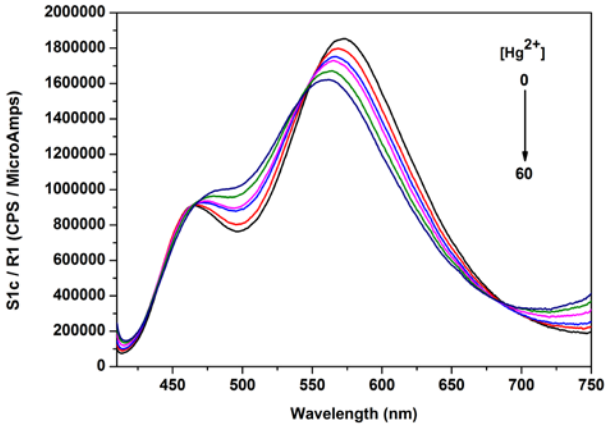

Figure S30. Fluorescence spectra of probe **L3** (60 μM) upon titration by Hg^{2+} ion (0-60 μM by 2 µM step) in 5% ACN:water mixture, (λ_{exc} = 400 nm; λ_{emi} = 572 - 561 nm, $\Delta\lambda_{emi}$ = 11 nm, Slit: 5 nm/5 nm).

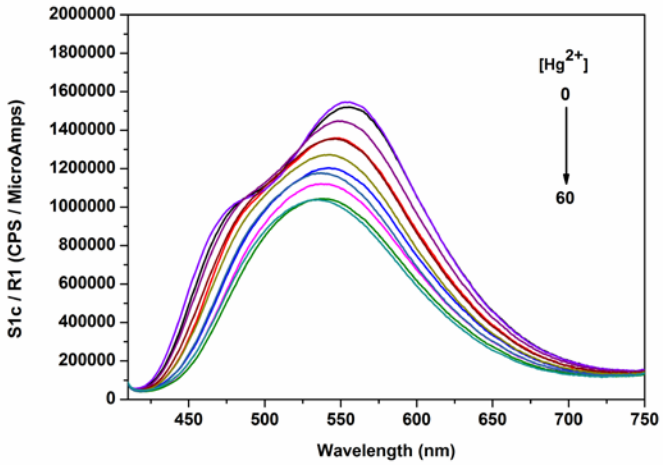

Figure S31. Fluorescence spectra of probe **L4** (60 μM) upon titration by Hg^{2+} ion (0-60 μM by 2 µM step) in 5% ACN:water mixture, (λ_{exc} = 400 nm; λ_{emi} = 553 - 536 nm, $\Delta\lambda_{emi}$ = 17 nm, Slit: 5 nm/5 nm)

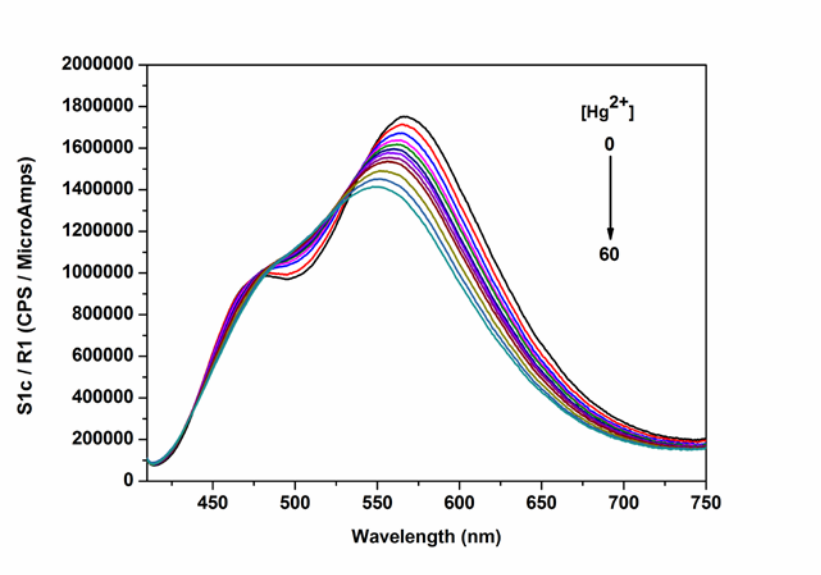

Figure S32. Fluorescence spectra of probe **L5** (60 μM) upon titration by Hg^{2+} ion (0-60 μM by 2 µM step) in 5% ACN:water mixture, (λ_{exc} = 400 nm; λ_{emi} = 565 - 553 nm, $\Delta\lambda_{emi}$ = 12 nm, Slit: 5 nm/5 nm)

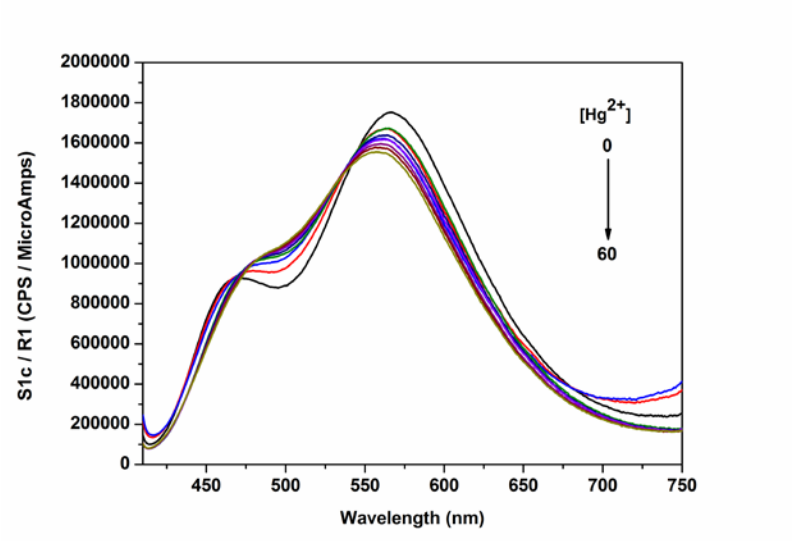

Figure S33. Fluorescence spectra of probe **L6** (60 μM) upon titration by Hg^{2+} ion (0-60 μM by 2 µM step) in 5% ACN:water mixture, (λ_{exc} = 400 nm; λ_{emi} = 566 - 558 nm, $\Delta\lambda_{emi}$ = 8 nm, Slit: 5 nm/5 nm)

8. ESI-MS analysis of the binary and ternary complexes

General procedure for preparation of sensing probe L1

Stock solutions of per-6-ABCD (**1b**) (0.0282 g) and 3-Hydroxy-*N*-phenyl-2-naphthamide (**2**) (0.0066 g) were prepared separately in 250 mL SMF. Aqueous solution of the per-6-ABCD:3-Hydroxy-*N*-phenyl-2-naphthamide complex, [**1b**:**2**] (probe **L1**) was prepared *in situ* from the reaction of **1b** (1 x 10^{-4} M) and **2** (1 x 10^{-4} M) by sonication for 6 h. **1b**:**2** complex (probe **L1**) is called binary complex. Then, aqueous Hg^{2+} ion solution (1 x 10^{-4} M) was added and allowed to stir at room temperature for 6 h to generate the ternary complex (per-6-ABCD:3-Hydroxy-*N*-phenyl-2-naphthamide:Hg^{2+} complex, **1b**:**2**:Hg^{2+} complex). Then the binary and ternary complexes was diluted (10^{-7} M) and analyzed directly by ESI-MS. ESI-MS was performed in negative ion mode. The collision voltage and ionization voltage were -70 V and -4.5 kV, respectively, using nitrogen as atomization and desolvation gas. The desolvation temperature was set at 300 ºC. The scan range of mass spectrum was 300–2000 m/z. The relative amount of each component was determined from the LC–MS chromatogram, using the area normalization method.

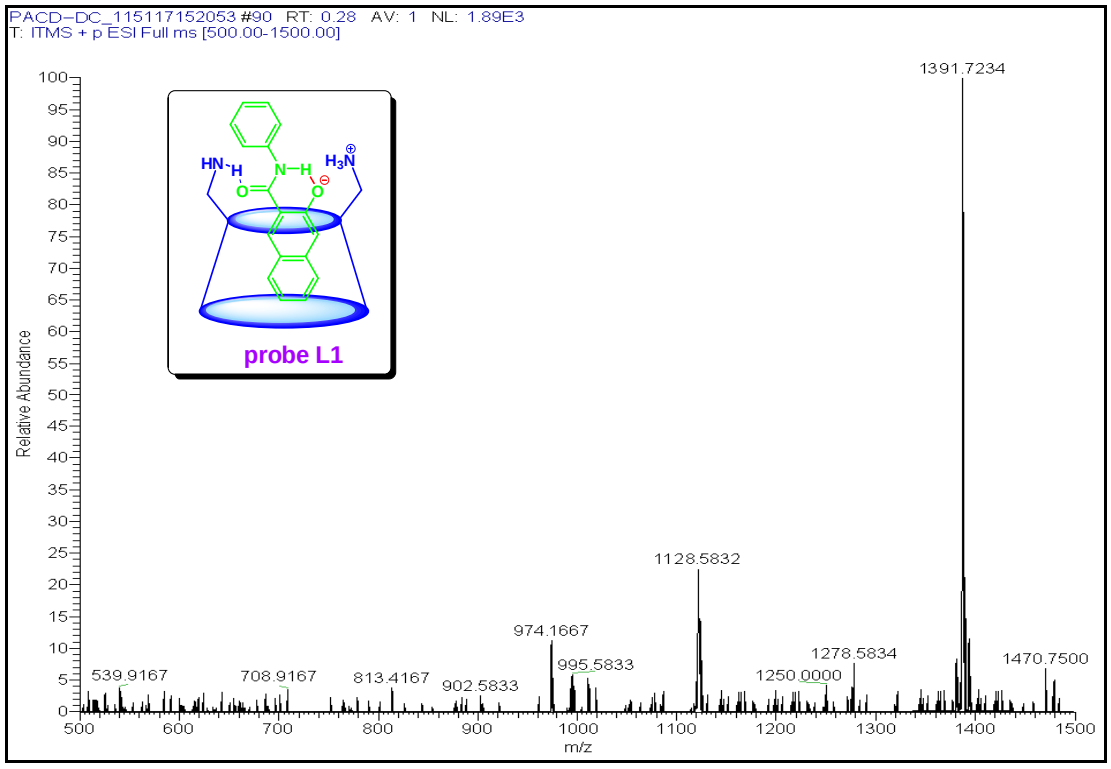

Figure S34. ESI-MS data of binary complex of per-6-ABCD:3-Hydroxy-*N*-phenyl-2-naphthamide, **1b**:**2** complex (probe **L1**) in water.

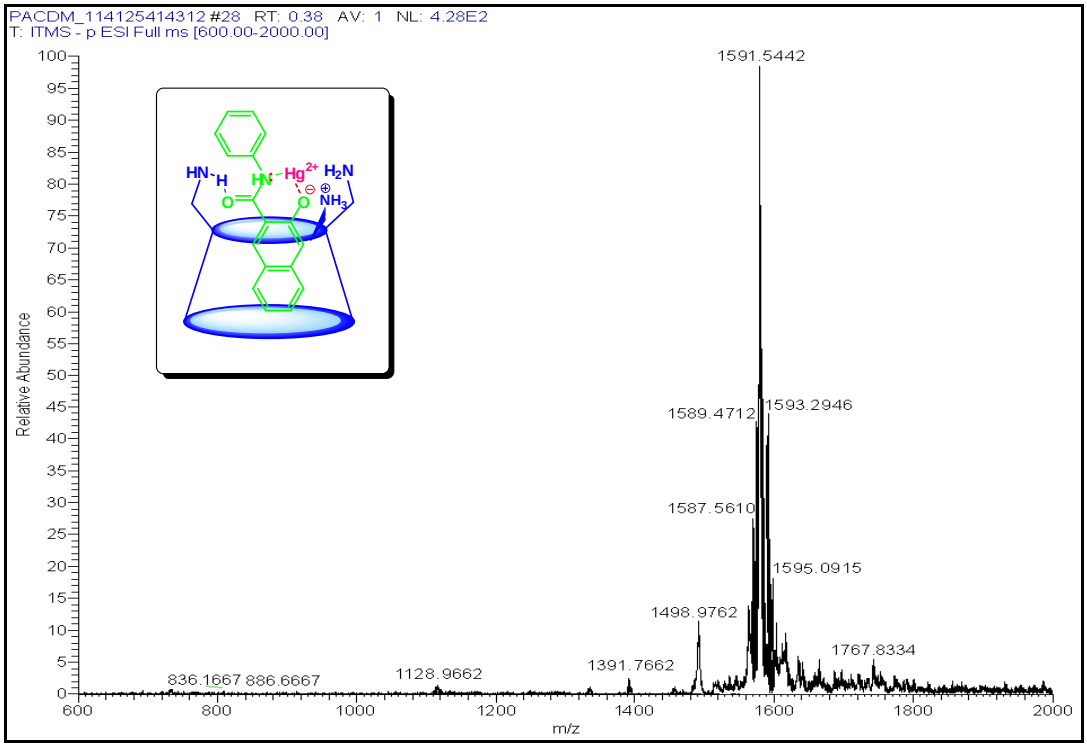

Figure S35. ESI-MS data of ternary complex of per-6-ABCD:3-Hydroxy-*N*-phenyl-2-naphthamide:Hg^{2+}, **1b**:**2:**Hg^{2+} complex in water.

9. pH Dependence sensing response of probe L1

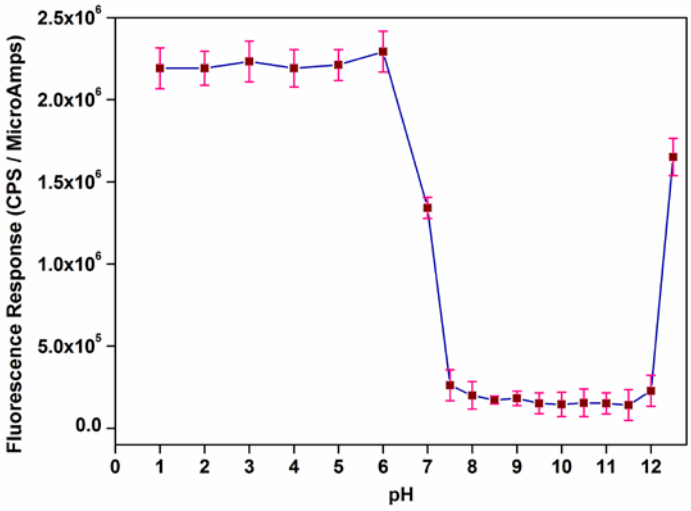

Figure S36. pH Dependence sensing behavior of the probe **L1** with Hg^{2+} ion (pH is maintained using HCl and NaOH).

10. Lifetime measurement studies

Single Photon Counting Spectrometer (TCSPC)

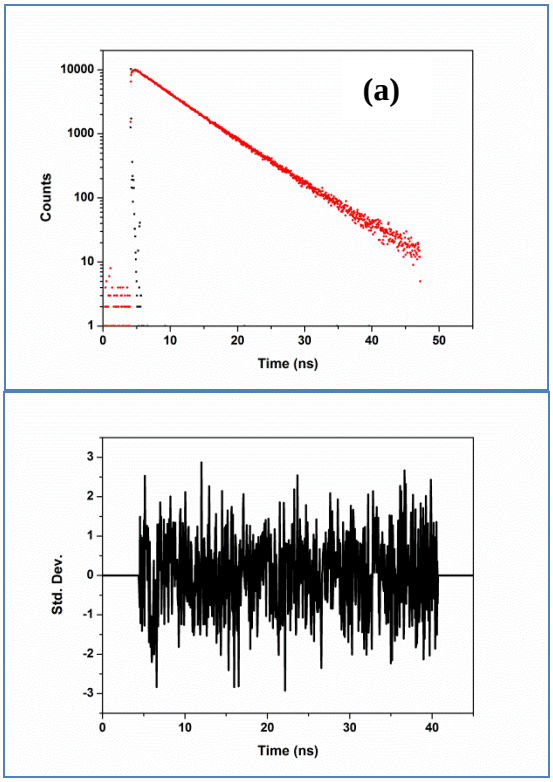

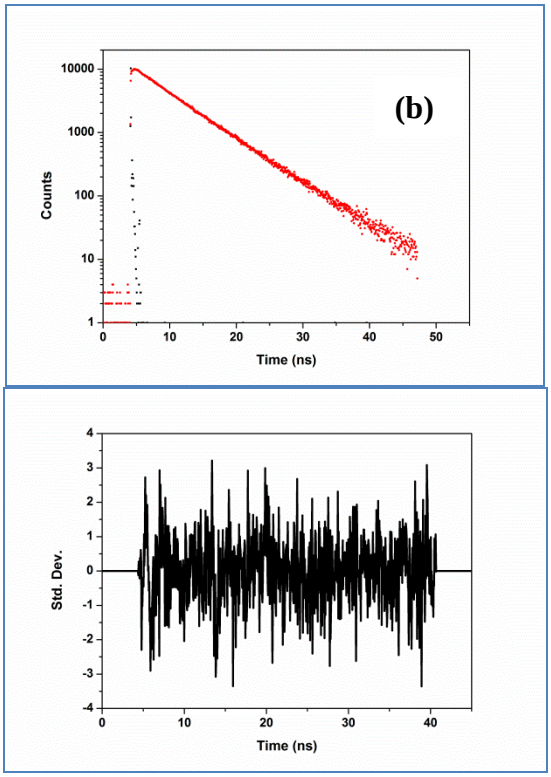

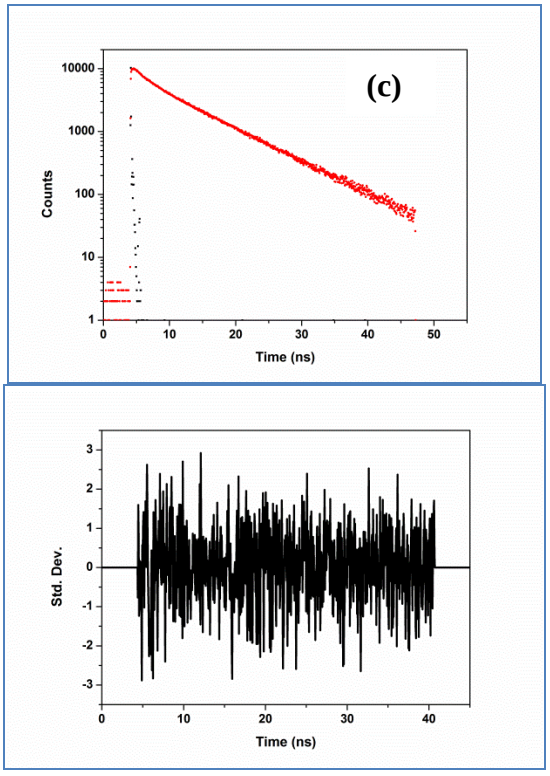

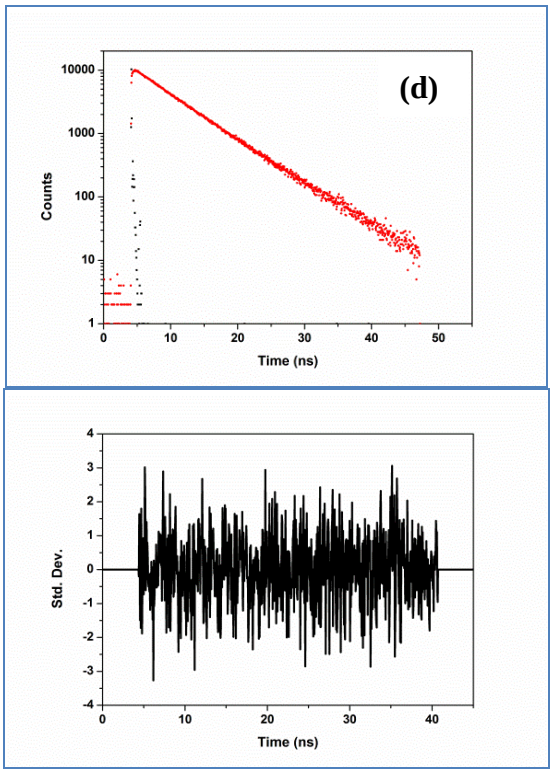

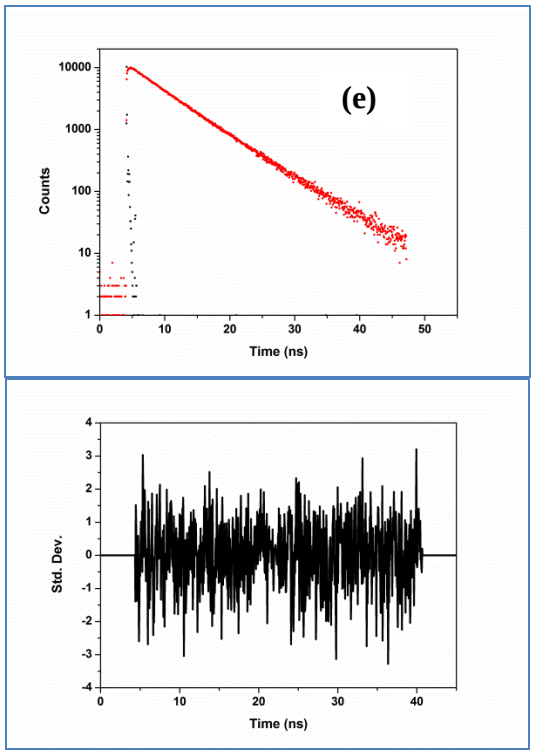
(e)
Counts
Time (ns)
Std. Dev.
Time (ns)

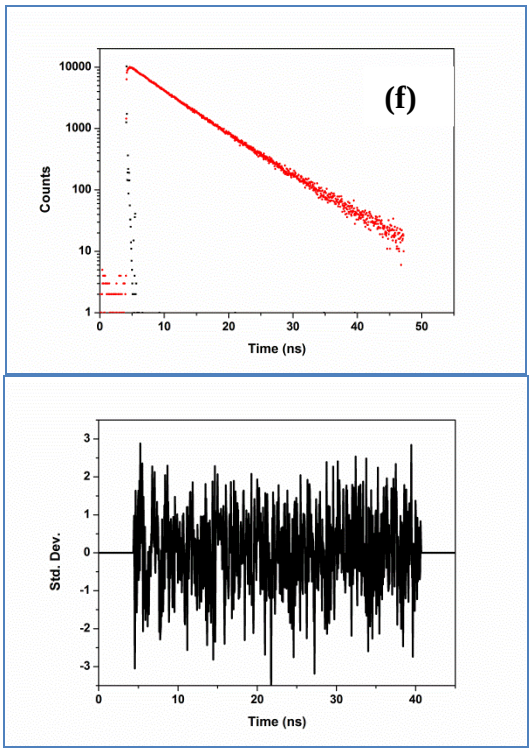
(f)
Counts
Time (ns)
Std. Dev.
Time (ns)

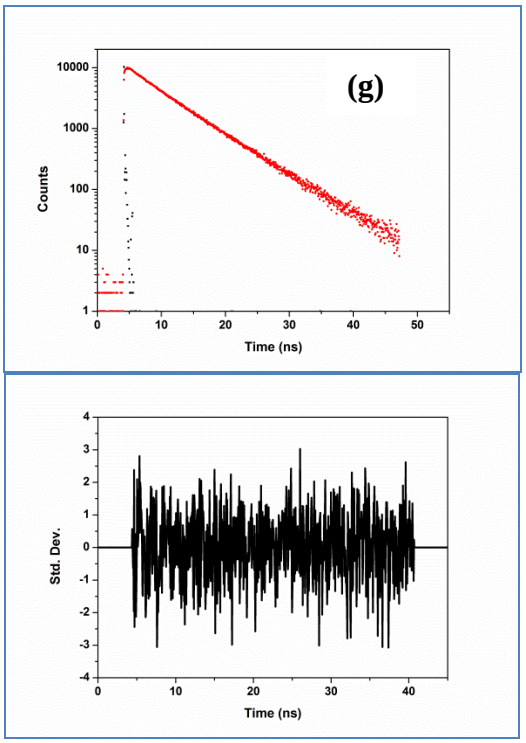
(g)
Counts
Time (ns)
Std. Dev.
Time (ns)

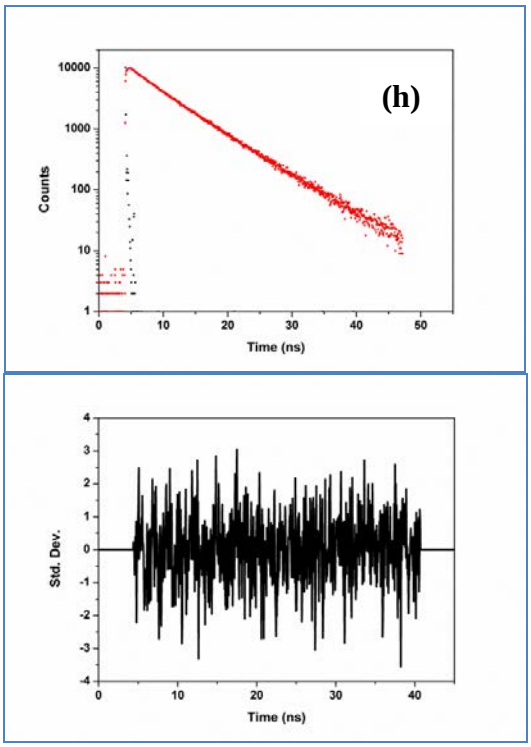
(h)
Counts
Time (ns)
Std. Dev.
Time (ns)

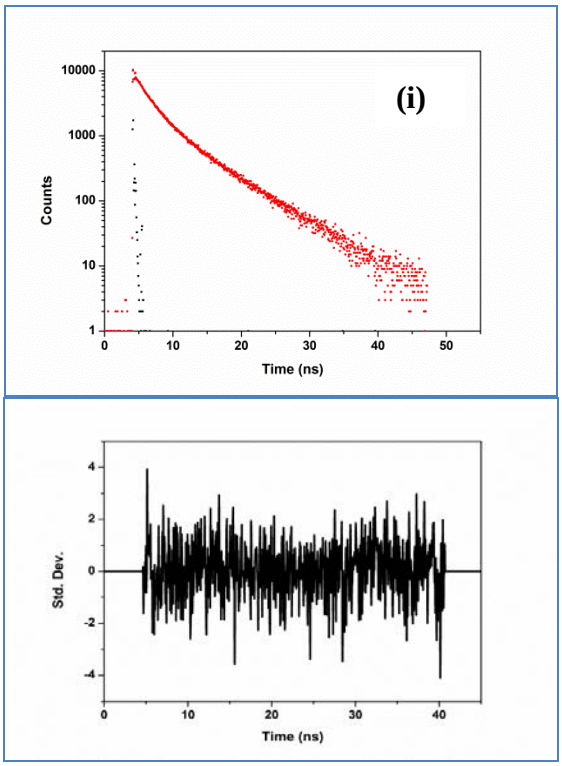

Figure S37. Fluorescence life-time exponential curves and standard deviation plots for (a) **2** ; (b) probe **L1**; (c) **L1** + Hg^{2+} (0.1 eqi.); (d) **L1** + Hg^{2+} (0.2 eqi.); (e) **L1** + Hg^{2+} (0.4 eqi.); (f) **L1** + Hg^{2+} (0.6 eqi.); (g) **L1** + Hg^{2+} (0.8 eqi.); (h) **L1** + Hg^{2+} (1.0 eqi.); (i) **L1** + Hg^{2+} (1.1 eqi.).

11. References

S1. Politi, M. J.; Tran, C. D.; Gao, G. H. *J. Phys. Chem.*, **1995**, *99*, 14137.

S2. Benesi, H. A.; Hildebrand, J. H. *J. Am. Chem. Soc.*, **1949**, *71***,** 2703

S3. (a) Casey, K. G.; Quitevis, E. L. *J. Phys. Chem.*, **1988**, *92*, 6590; (b) http://www.jobinyvon.co.uk/SiteResources/Data/MediaArchive/files/Fluorescence/applications/quantumyieldstrad.pdf; (c) J. Q. Umberger, V. K. Lamer, *J. Am. Chem. Soc.*, **1945**, *67*, 1099.

S4. Ashton, P. R.; Koniger, R.; Stoddart, J. F. *J. Org. Chem.* **1996**, *61*, 903.

S5. Zhang, X.; Guo, L.; Wu, F.-Y.; Jiang, Y. B. *Org. Lett.*, **2003**, *5*, 2667.

S6. Choe, J. I.; Kim, K.; Chang, S. K. *Bull. Korean Chem. Soc.* **2000**, *21*, 200.

S7. Choe, J. I.; Chang, S. K. *Bull. Korean Chem. Soc.* **2002**, *23*, 48.

S8. Discover User Guide, Accelrys, **2001**.

S9. M. J. Frisch, G. W. Trucks, H. B. Schlegel, G. E. Scuseria, M. A. Robb, J. R. Cheeseman, J. A. Jr. Montgomery, T. Vreven, K. N. Kudin, J. C. Burant, J. M. Millam, S. S. Iyengar, J. Tomasi, V. Barone, B. Mennucci, M. Cossi, G. Scalmani, N. Rega, G. A. Petersson, H. Nakatsuji, M. Hada, M. Ehara, K. Toyota, R. Fukuda, J. Hasegawa, M. Ishida, T. Nakajima, Y. Honda, O. Kitao, H. Nakai, M. Klene, X. Li, J. E. Knox, H. P. Hratchian, J. B. Cross, V. Bakken, C. Adamo, J. Jaramillo, R. Gomperts, R. E. Stratmann, O. Yazyev, A. J. Austin, R. Cammi, C. Pomelli, J. W. Ochterski, P. Y. Ayala, K. Morokuma, G. A. Voth, P. Salvador, J. J. Dannenberg, V. G. Zakrzewski, S. Dapprich, A. D. Daniels, M. C. Strain, O. Farkas, D. K. Malick, A. D. Rabuck, K. Raghavachari, J. B. Foresman, J. V. Ortiz, Q. Cui, A. G. Baboul, S. Clifford, J. Cioslowski, B. B. Stefanov, G. Liu, A. Liashenko, P. Piskorz, I. Komaromi, R. L. Martin, D. J. Fox, T. Keith, M. A. Al-Laham, C. Y. Peng, A. Nanayakkara, M. Challacombe, P. M. W. Gill, B. Johnson, W. Chen, M. W. Wong, C. Gonzalez, J. A. Pople, Gaussian 03, revision E.01; Gaussian, Inc.: Wallingford, CT, **2004**.